REPURPOSING 13-CIS-RETINOIC ACID: A POTENTIAL TREATMENT FOR ANEURYSMS-OSTEOARTHRITIS SYNDROME

By Samantha Putos

This thesis is submitted as a partial fulfillment of the M.Sc. program in Cellular and Molecular Medicine.

May 5 2015

University of Ottawa
Ottawa, ON

Preliminary Pages

Abstract

Approximately 7000 rare disorders exist, affecting 2 percent of Canadians and millions of people worldwide. Given that for many rare diseases only one allele is mutated, we hypothesize inducing expression of the remaining wild-type allele may have a therapeutic effect. *SMAD3* heterozygosity results in Aneurysms-Osteoarthritis Syndrome (AOS) – an aortic aneurysm disorder also known as Loeys-Dietz Syndrome Type 3. We conducted a screen of FDA-approved compounds and found that 13-cis-retinoic acid (13-CRA) induces *SMAD3* in normal human fibroblast cultures. Treatment with therapeutic concentrations of 13-CRA increased *SMAD3* mRNA in normal human fibroblasts, patient fibroblasts, wild-type murine vascular smooth muscle cells and *Smad3*+/- murine vascular smooth muscle cells. Increases in SMAD3 protein were also observed in normal human fibroblasts, patient fibroblasts, and wild-type murine vascular smooth muscle cells. Immunofluorescent imaging revealed the primary site of protein induction to be nuclear. We report here the *in vitro* induction of *SMAD3* mRNA and protein by therapeutic levels of 13-CRA and suggest further investigation of this modality for the treatment of AOS.

Table of Contents

List of Tables

List of Figures

List of Abbreviations

°C	Degrees Celsius
µg	Micrograms
µl	Microliter
µM	Micromolar
13-CRA:	13-cis-retinoic acid
ALK1:	Activin receptor-like kinase 1
AOS:	Aneurysms-osteoarthritis syndrome
BMP-2:	Bone morphological protein 2
bZIP:	Basic leucine zipper
C/EBPβ:	CCAAT/Enhancer binding protein beta
C4R:	Care for Rare
cDNA:	Complementary DNA
CHEO:	Children's Hospital of Eastern Ontario
CMAP:	Connectivity map
Co-SMAD:	Collaborating SMAD
DAPI:	4',6-diamidino-2-phenylindole
DMEM:	Dulbecco's Modified Eagle's Medium
DMSO:	Dimethylsulfoxide
DNA:	Deoxyribonucleic acid
ECM:	Extracellular matrix
ENG:	Endoglin
FBN-1:	Fibrillin-1

FDA:	Food and Drug Administration
FORGE:	Finding of Rare Disease Genes
GAPDH:	Glyceraldehyde 3-phosphate dehydrogenase
GEO:	Gene Expression Omnibus
h:	Hours
HHT:	Hereditary haemorrhagic telangiectasia
HPRT1:	Hypoxanthine phosphoribosyltransferase 1
HSC:	Heat shock cognate
IP:	Intraperitoneal
kb:	Kilobase
kDa:	Kilodalton
LDS:	Loeys-Dietz Syndrome
LDS3:	Loeys-Dietz Syndrome Type 3
MFS:	Marfan Syndrome
MH1:	Mad homology 1
MH2:	Mad homology 2
NCBI:	National Center for Biotechnology Information
NHF:	Normal human fibroblast
nM:	Nanomolar
NMD:	Nonsense-mediated decay
OMIM:	Online Mendelian Inheritance in Man
PBS:	Phosphate buffered saline
PFA:	Paraformaldahyde

R-SMAD:	Receptor-activated SMAD
RA:	Retinoic acid
RAR:	Retinoid acid receptor
RARE:	Retinoic acid response element
RIPA:	Radioimmunoprecipitation assay
RNA:	Ribonucleic acid
RXR:	Retinoic X receptor
SARA:	Smad anchor for receptor protein
SEM:	Standard error of the mean
SMAD2:	Small mothers against decapentaplegic homolog 2
SMAD3:	Small mothers against decapentaplegic homolog 3
SMAD4:	Small mothers against decapentaplegic homolog 4
$t_{1/2}$:	Half-life
TGF-β:	Transforming growth factor β
VSMC:	Vascular smooth muscle cell
WT:	Wild-type

Acknowledgements

This thesis is the product of contributions from several individuals. First and foremost I would like to thank my supervisor, Dr. Alex MacKenzie, for his tireless patience, dedication, and enthusiasm for my project and support towards my future career endeavors. Thanks so much for everything you've done for me!

Second, I would like to say thank you to the members of the MacKenzie lab for creating a welcoming environment in which to work every day, and to all the members of CHEO RI who have helped me with various aspects of my project. I am honoured to have had the opportunity to learn from such a wonderful group of passionate scientists. Special thanks to Dr. Kristin Kernohan for help with the immunofluorescence experiments.

I would like to thank my boyfriend Nick and my sister Heather for their listening ears and words of encouragement during the most challenging times over the last two years. To my wonderful parents: I do not underestimate how fortunate I am to have your unwavering support through my sporadic and ongoing flurry of ideas in trying to find the right career path.

Finally, there are two individuals without whom I truly would not have been able to complete this thesis. I would like to extend my most sincere gratitude to Dr. Jason Vanstone for his continued guidance, support, mentorship, and comic relief throughout my project. Your daily feedback, advice, and assistance were invaluable. To Dr. Alan Mears, I cannot express enough my appreciation for all of your help and expertise – for doing the FDA drug screen and preliminary work on the Isotretinoin experiments, for doing the dosing and blinding for my *in vitro* studies, and for providing insightful

feedback on all aspects of my project every step of the way. I could not have done it without you!

INTRODUCTION

General Introduction

At present approximately 7000 diseases are classified as rare, meaning less than 1 in 2000 people are affected[1]. While individually rare these disorders are collectively common, affecting 2 percent of Canadians and millions of people worldwide[2]. Many rare disorders result in poor quality of life for both patients and their families and impose significant burden on the health care system. Unfortunately, therapy development for rare diseases is largely neglected by researchers and pharmaceutical companies due to limited understanding of disease etiology, lack of public awareness and funding, limited subject availability for clinical trials, and the small profit margin on developing novel agents that are sought by so few patients[3].

Aneurysms-Osteoarthritis Syndrome (AOS), also known as Loeys-Dietz Syndrome Type 3 (LDS3), is one such rare disease for which there is no current cure. AOS is characterized by aggressive aneurysms of the ascending aorta and early onset-osteoarthritis. Patients and their families face a bleak prognosis, limited treatment options, and uncertain life expectancy. With the recent delineation of AOS genetic etiology, we believe that underlying genetic dysfunction can be modulated with the use of small molecules. This report focuses on repurposing a widely used FDA-approved compound, 13-cis-retinoic acid (13-CRA), for the potential treatment of AOS.

Loeys-Dietz Syndrome

Dr. Bart Loeys and Dr. Harry Dietz at John Hopkins University first characterized Loeys-Dietz Syndrome (LDS) in 2005. Since this time four types of LDS have been described, classified by genetic etiology and named types 1-4. Aneurysms are common to all types and are typically found in the ascending aorta but can also develop throughout the arterial tree. LDS types 1 and 2 (OMIM #609192, #610168) form a clinical continuum and are characterized by autosomal dominant mutation to transforming growth factor beta (TGF-β) receptor 1 and TGF-β receptor 2, respectively. LDS type 4 (OMIM ##614816) is caused by mutation to the ligand TGF-β2 and tends to have a slightly milder phenotype[4]. In addition to aneurysms of the ascending aorta, LDS Type 1, 2, and 4 patients may have hypertelorism (widely spaced eyes), bifid uvula, cleft palate, and arterial tortuosity. The mean age of death, typically due to aneurysmal rupture, is 26[5]. Other manifestations may include craniosynostosis, brain abnormalities, mental retardation, and heart disease[4]. There is no explicit timeline for the progression of LDS; aneurysms have been detected as early as 19 weeks of age *in utero* via ultrasound imaging[6], and infantile dissections have been reported as young as 3 months of age[7]. In general, individuals with more severe craniofacial abnormalities tend to experience aneurysm rupture at an earlier age and at smaller dimensions[4, 8]. Due to highly variable symptoms, diagnosis of LDS must be made using genetic testing. Individuals with LDS type 2 are depicted in Figure 1.

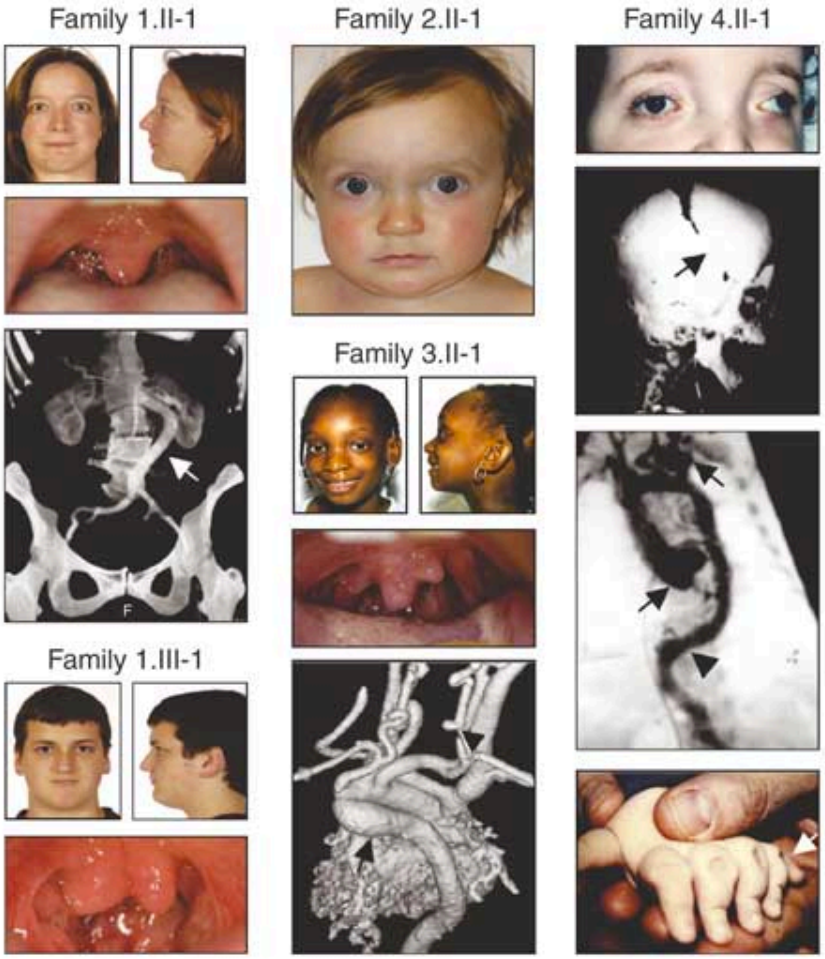

Figure 1. The spectrum of phenotypes caused by mutations in TGFβ Receptor 2. Individual II-1 in family 1 (1.II-1) shows hypertelorism, malar flattening and a broad-based uvula. Imaging showed a tortuous abdominal aorta (arrow). Her son, individual 1.III-1, shows malar flattening and a bifid uvula. Individual 2.II-1 shows hypertelorism. Individual 3.II-1 shows hypertelorism, bifid uvula, a proximal descending aorta that makes a full hairpin turn (arrow) and pig-tail loops of the carotid arteries (arrow head). Individual 4.II-1 shows marked hypertelorism, outward deviation of the left eye (exotropia), premature fusion of the coronal suture of the skull (arrow), marked tortuosity of the aorta (arrow head), aortic root and subclavian artery aneurysms (arrows) and a sixth digit on the left hand (arrow). Figure and legend reprinted by permission from Macmillan Publishers Ltd: Nature genetics [4] © 2005.

In contrast to other forms of the condition, AOS (OMIM #613795) patients exclusively manifest mutations in the Small Mothers Against Decapentaplegic homolog 3 (*SMAD3)* gene. These patients also develop aneurysms prone to dissection, but ruptures usually occur later in life than in other LDS disorders. As the name suggests, a high percentage of patients develop early-onset osteoarthritis. This is commonly the symptom that leads patients to seek medical attention leading to AOS diagnosis[9]. AOS patients tend to lack craniofacial and psychological abnormalities typical of other aneurysm disorders, instead displaying only mild or benign findings (*e.g.* arachnodactyly – abnormally long fingers relevant to the size of the palm). This makes the disease difficult to detect; without a recognized family history, AOS may simply go undiagnosed. Facial features of several AOS patients are depicted in Figure 2.

Aneurysms Osteoarthritis Syndrome

AOS was first described in 2011 when the effects of *SMAD3* heterozygosity were first distinguished from those of TGF-β. In the study by van de Laar *et al*. where the name AOS was first proposed, three Dutch families with aortic aneurysms, arterial tortuosity, and a history of sudden death between the ages of 39 and 65 were investigated[9]. Most of the cases presented with early-onset osteoarthritis and several had other congenital heart diseases, but craniofacial and psychological abnormalities were mild or absent. The study identified two putatively pathogenic *SMAD3* mutations: a substitution of arginine for tryptophan at position 287 of *SMAD3*, and a deletion of 2 nucleotides in exon 6 causing a frameshift and consequential stop codon in exon 7. Using cyclohexamide (an inhibitor of nonsense-mediated decay) and primers specific to each

Figure 2. Facial features of 20 patients with AOS from four different families. Related patients are grouped by coloured box borders. Figure and legend reprinted by permission from Macmillan Publishers Ltd: Journal of Medical Genetics [10] © 2011.

SMAD3 allele, the study showed that mutant transcripts are rapidly degraded in patient cell lines and that the protein product from the mutant allele is not formed[9]. This data suggests that the mutations result in *SMAD3* haploinsufficiency.

Since its definition in 2011, several other reports have been published describing AOS patients with a range of symptoms and novel *SMAD3* mutations. In a separate study, van de Laar *et al*. identified 5 novel *SMAD3* mutations in a cohort of aneurysm patients without TGF-β receptor 1 or TGF-β receptor 2 mutations. Out of 45 patients with *SMAD3* mutation, all exhibited one or more symptoms of AOS; they therefore concluded that the penetrance of *SMAD3* mutation is almost 100%[10]. AOS findings are largely age-dependent. The youngest patient in the study was 9 years of age and only exhibited a bifid uvula. The youngest patients to have an aortic aneurysm were 14 and 16 years of age, and the youngest patient with aneurysm dissection was 34 years of age. The most serious findings (multiple aneurysms with dissections) occurred in a 50-year old patient[10].

In 2012, Regalado *et al*. identified additional heterozygous *SMAD3* mutations in exons 2, 5, and 6 in families with a history of aneurysms[11]. In one family, a frameshift mutation was identified that resulted in ascending aortic and intracranial aneurysms, as well as abdominal aortic and bilateral iliac artery aneurysms. They discovered 3 additional *SMAD3* mutations in 4/181 probands and concluded that *SMAD3* mutations are responsible for 2% of familial thoracic aortic aneurysms and dissections[11]. Later that same year, yet another *SMAD3* mutation was identified in several family members with a large deletion on chromosome 15 that eliminated the entire coding region of *SMAD3* with the exception of exon 1[12]. In contrast to initial reports, emerging studies reported a

variable phenotype ranging from completely normal to significant mental retardation. However, AOS symptoms are still generally described as less severe than those in LDS.

Aneurysm Development and TGF-β Pathway

The maintenance of blood vessel walls is a dynamic process that balances deposition and degradation of vascular smooth muscle cell (VSMC) extracellular matrix (ECM)[13, 14]. In contrast to "sporadic" non-monogenic aortic aneurysms, which typically occur in the descending aorta, AOS patients develop aneurysms of the ascending aorta that are not caused by atherosclerotic plaque buildup[15, 16]. Histological analyses of aortic tissue from patients with AOS, LDS and Marfan Syndrome (MFS, OMIM #154700, another ascending aortic aneurysm disorder) show both a loss of elastin protein and a dissociation of elastin deposits from VSMCs in the aortic wall[4, 9]. The specimens show a lack of inflammation suggesting that it is a defect in elastogenesis, and not injury to the area, that has caused this deficiency and separation[4]. Loss of elastin fibers causes vessels to stiffen and dilate under high-pressure and turbulent blood flow. Dilated vessels are prone to small tears in the inner endothelium, which allow blood to flow between vessel wall layers; this constitutes a dissection, leading to an increased risk for rupture.

Only recently has the importance of the TGF-β pathway and its effectors been identified in this pathology[4, 17, 18]. Prior to 2005, LDS patients were often misdiagnosed with MFS, a connective tissue disorder caused by mutation to fibrillin-1 (*FBN-1*) gene that affects the eye, skeleton, and aorta[19]. While LDS has some similarities to MFS such as aortic aneurysms and skeletal malformations, it was clear that a subgroup of MFS patients exhibited a markedly more severe phenotype. Genetic

sequencing soon after confirmed a distinct disorder caused by mutation to the TGF-β receptor. This discovery led researchers to consider the possibility of a role for perturbation of the TGF-β pathway in aneurysm development[20]. Before, loss of vessel elasticity and dislocation of the ocular lens in MFS could be attributed to deficiency in fibrillin-1, but other prominent skeletal manifestations such as scoliosis could not be explained. New knowledge of the TGF-β mutation in LDS prompted investigation of TGF-β levels in MFS mice, which were found to be elevated in affected tissues. This ultimately led to a better understanding of disease pathology for both MFS and other disorders of the ascending aorta.

Numerous reports have now noted elevated TGF-β signaling in LDS, AOS and MFS patient tissues/cells[4, 8, 9, 21]. Downstream targets of TGF-β such as SMAD2, SMAD3, collagen and connective tissue growth factor are also increased[4]. While the causative mutation in each disorder is distinct, increased TGF-β signaling is thought to be a common driving factor in aneurysm development. In MFS, mutated *FBN-1* gene results in defective fibrillin protein. Fibrillin monomers exist in VSMC ECM as aggregates, on which elastin fibers are synthesized[22]. Epidermal growth factor-like motifs in fibrillin proteins contain calcium-binding sequences, which sequester calcium to protect against ECM proteolysis and help maintain lateral packing of microfibrils[23, 24]. Mutated fibrillin is unable to adequately sequester calcium, allowing for enhanced breakdown of the ECM, disorderly packing of elastin fibers, and degradation of the microfibril network that supports vessel walls. Fibrillin-rich microfibers are also known to sequester latent TGF-β complexes within the ECM[22]. In order to be activated, TGF-β must be released from sequestration by fibrillin. Dysfunctional fibrillin microfibrils allow more TGF-β to

be available for activation, leading to enhanced TGF-β signaling[25]. In LDS, gain of function mutation to the TGF-β receptor is responsible for hyper-activation of TGF-β pathway. In AOS, it is thought that deficiency in the downstream effector SMAD3 results in compensatory TGF-β expression. There is a growing body of evidence that suggests TGF-β can bypass traditional signaling pathways to activate downstream targets. In particular, several studies have documented the ability of TGF-β to propagate type 1 receptor signals in the absence of SMAD activity[26-30]. Thus, if SMAD3 protein is low, compensation by TGF-β may be affecting downstream targets via both SMAD-mediated and alternate pathways.

Experiments on heterozygous *FBN*-1 mice show that treatment with a systemic TGF-β neutralizing antibody rescues aortic, lung, and skeletal muscle phenotypes[18]. This finding indicates that increased TGF-β signaling is not secondary to disease progression, but is indeed driving the development of aneurysms. It is now widely accepted that the surplus of activated TGF-β is directly responsible for degradation of VSMC ECM in aneurysm development[22], suggesting it is not a deficiency of SMAD3 that is directly responsible for vascular remodeling in AOS, but rather consequences of TGF-β compensation. We hypothesize that restoring levels of SMAD3 may abrogate TGF-β signaling, reestablishing ECM balance and potentially halting aneurysm progression.

SMAD3 Gene

The *SMAD3* gene has 9 exons and spans 129 kb of genomic DNA, mapping to the long arm of chromosome 15[31, 32]. *SMAD3* is one of nine SMAD molecules, so named for their homology to *sma* and *Mad* genes in *C. elegans* and *Drosophila*. SMADs were

the first substrates of type 1 (serine/threonine kinase) receptors identified, and continue to be recognized as the only well-characterized downstream effectors of TGF-β[33]. SMADs are central in transmitting signals to the nucleus and influence cell cycle regulation, differentiation, and apoptosis[34]. Multiple reports have indicated specific tumor-suppressor roles of *SMAD3* and linked its mutation to cancer[35, 36], making it the subject of investigation for many cancer-related studies. However, while several studies have investigated the *downstream* targets of SMAD3, little is known about its *upstream* modulators.

There are four *SMAD3* isoforms. Alternative transcripts usually exclude one or more exons, and the resulting protein lacks some activity (*e.g*. *SMAD3*Δexon3 lacks DNA binding ability)[37]. The terminals of SMAD molecules are well conserved across species, but the linker region between them is highly variable in both size and sequence[33]. The N-terminus and C-terminus are referred to as MH1 and MH2 domains, respectively. It is thought that the MH1 domain both interacts with and inhibits the activity of MH2 in a basal state, and has DNA-binding capability in the activated state[33]. The MH2 domain mediates SMAD3 interaction with type 1 receptors, and contains highly conserved phosphorylation sites. These are in the form of an SSXS (Ser-Ser-X-Ser) motif, the 2-most C-terminal serine residues of which are phosphorylated during activation[38, 39]. Figure 3 depicts the structures of SMAD molecules.

In a basal state, SMAD3 exists in the cytoplasm as homo-oligomers supported by the MH2 domain and parts of the linker region. It is also bound by Smad anchor for receptor protein (SARA), which keeps SMAD3 in the cytoplasm by obstructing a nuclear

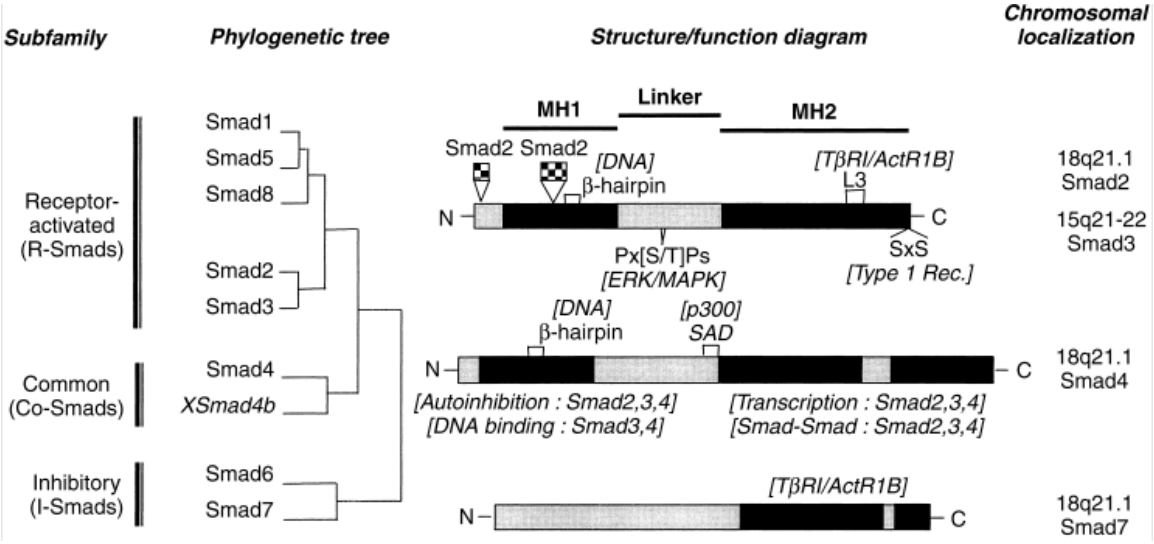

Figure 3. Phylogenic tree of vertebrate Smads (except Xenopus Smad4b) and structure/function diagram. MH1 and MH2 indicate *Mad* homology region 1 and 2, respectively. Reprinted by permission from Macmillan Publishers Ltd: Kidney International Supplements – Nature [40], copyright (2000).

import signal in the MH2 domain[41], and also facilitates SMAD3 presentation to activated type 1 receptors[42]. When TGF-β binds type 2 receptors they heterodimerize to type 1 receptors and phosphorylate the MH2 domain of SMAD3, diminishing its affinity for SARA and exposing the nuclear import signal[43-45]. Because SMAD3 activation is dependent on TGF-β receptor, it is considered a receptor-activated SMAD (R-SMAD)[33]. Once phosphorylated, R-SMADs may bind to the collaborating SMAD (Co-SMAD) SMAD4 and enter the nucleus, although this binding is not required for SMAD3 nuclear entry[46]. In the nucleus, full-length SMAD3 is able to directly bind DNA at the TGF-β response element CAGA, which is mediated by a β-hairpin motif in the MH1 domain[47]. Although SMAD3 can directly bind DNA independently, its affinity for the TGF-β response element is low and therefore usually requires DNA binding cofactors[47]. SMAD3 has numerous target genes and can is known to act as both an activator and repressor. Figure 4 provides a basic illustration of R-SMADs in the TGF-β pathway.

All known *SMAD3* mutations causing AOS result in disruption or deletion of the MH2 activation region. Some mutations are within the activation region, while others are further upstream and result in a truncated transcript. In either case, the mutant transcripts are likely subject to nonsense-mediated decay (NMD)[9] or form a protein product that cannot be activated and is unable to enter the nucleus. To correct this, we hypothesize restoring levels of functional SMAD*3* protein by stimulating expression of the wild-type (WT) *SMAD3* allele with the use of small molecule modulators.

.

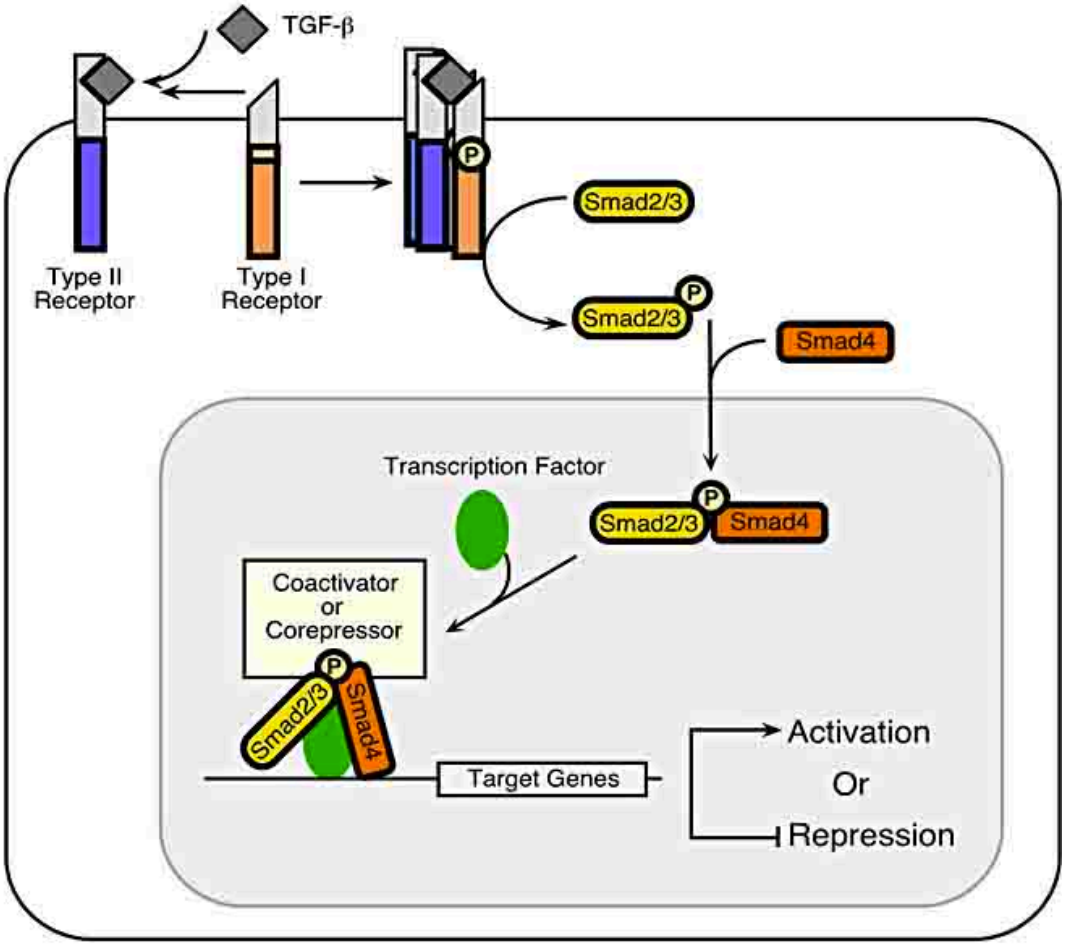

Figure 4. TGF-β/R-SMAD signaling pathway overview. TGF-ß binding results in the formation of a ligand-receptor complex and activation of the type I receptor. The activated type I receptor then phosphorylates Smad2 and Smad3. Smad4 complexes with phosphorylated Smad2 and Smad3, which accumulate in the nucleus. Smad3 and Smad4 possess DNA binding activities, whereas Smad2 cannot bind to DNA. Figure and legend adapted from Liu, 2003[48].

Care for Rare

Although the situation is improving, there still exists a lack of both research and pharmaceutical efforts to find treatments for rare diseases. In 2013, the Care for Rare (C4R, http://care4rare.ca/) project was initiated to help fill this void. C4R is a collaborative Canadian effort by researchers and clinicians to improve clinical care for patients and families affected by rare disease. C4R is a continuation of the Finding of Rare Disease Genes (FORGE) Canada project and aims to improve diagnoses and treatment of rare disorders. Led by Dr. Alex MacKenzie and Dr. Kym Boycott at the Children's Hospital of Eastern Ontario (CHEO), C4R has 16 co-applicants and numerous end-users from institutions across Canada. The project is divided into four Activities, each with a specific set of research or clinical objectives. Among these, Activity 3 involves the re-positioning of clinic-ready compounds to treat rare disease.

Rationale

Humans inherit the majority of their 22 000 functional genes in duplicate – one allele from each parent – and two functional copies are often required for normal development. A number of rare diseases arise when one allele is mutated, despite the second allele remaining functional. In such cases, particularly when the causative mutation is null and does not cause a pathogenic gain of function, modulating levels of RNA transcription and/or protein translation from the normal or WT allele may have a therapeutic effect. Several small molecules have been identified as modulators of the human transcriptome[49], are approved by the Food and Drug Administration (FDA), and are ready for clinical application or already in use. By repositioning such compounds, a portion of the timely and costly clinical trials required to obtain FDA approval can be

bypassed. Thus, one goal of C4R Activity 3 is to identify genes that are both associated with rare disease and that are responsive to pharmacologic modulation by clinic-ready compounds.

From a larger list of disease-causing genes compiled from FORGE, as well as a roster of diseases present in CHEO patients, Drs. Alex MacKenzie and Kym Boycott selected approximately 80 clinically attractive genes for which to seek therapies. These were sorted into five categories: 1) Haploinsufficiency (one mutated allele is enough to cause the disease phenotype); 2) Paralogs (a gene similar to the causative gene exists that may have the potential to rescue the disease phenotype) 3) Hypomorphs (impaired gene function through reduced, but not completely ablated, expression and/or functionality); 4) Supplementation (genes encoding proteins that are known to respond to supplements such as zinc, vitamins, etc.); and 5) Miscellaneous (http://bioinformat.info/whitepages/). *SMAD3* can be found in the haploinsufficiency column (Table 1). Other C4R genes of interest associated with well-characterized rare disorders include SCN1A (Haploinsufficiency), mutation to which causes a dysfunctional neuronal sodium channel in Dravet Syndrome; LAMA2 (Paralogs) which codes for laminin 2 and is associated with merosin-deficient congenital muscular dystrophy; TYMP (Hypomorphs) which codes for a thymidine phosphorylase and is associated with mitochondrial DNA depletion syndrome 1; SLC16A2 (Supplementation), a thyroid hormone transporter which may cause monocarboxylate transporter 8 deficiency when mutated; and CASP8 (Miscellaneous) which codes for caspase 8 and is associated with caspase 8-deficiency.

Haplo-insufficiency	Paralogs	Hypomorphs		Supplementa-tion	Miscellane-ous
ATP1A2	ABCD1 (ABCD2)	HARS	HSD17B4	ZIP8	ACER2
AFG3L2	ZIP8 (SLC39A14)	SBDS	NEU1	GPR172A	ANO5
COL6A1	PINCH2 (LIMS1)	ASAH1	MAN2B1	CSF1R	RDH12
ASAH2	DMD (UTRN)	MMACHC	ATP7A	NMNAT1	SCN2A
FGF14	FBN1 (FBN2)	MUT	ATP7B	SLC6A8	CFLAR
ITPR1	LAMA2 (LAMA1)	BSCL2	SUMF1	LSC16A2	CASP8
MAPT		AGPAT2	GBE1		CASP10
MPZ		ADUA	HSD11B2		SCN3A
NKX2-1		IDS	GAA		
OPA1		SGSH	HPRT1		
PGRN		GLB1	CPT2		
PMP22		GALNS	BCKD		
SCN1A		GUSB	ASL		
SLC2A1		ACADVL	SCARB2		
SMAD3		ALDH18A1	OTC		
SPAST		ARSA	GALT		
		GALC	CLN3		
		ASPA	CLN1		
		EIF2B5	ETFA		
		POLR3A	FH		
		PLP1	TYMP		
		PMM2	CTSA		
		FKRP	HEX A		

		PHYH	HEX B		
		AGXT	SACS		
		AMACR			

Table 1. C4R genes by category.

FDA Drug Screen

The initial stage of Activity 3 was to establish potentially favourable interactions between clinic-ready compounds and genes associated with rare disease. Several techniques were used to identify compounds that might induce genes of interest; one of these was an FDA drug screen. From a library of over 800 FDA-approved drugs, approximately 310 that were safe for long-term use were selected. Harsh antineoplastic agents, antipsychotics, etc. were eliminated from the screen as C4R disorders are both congenital and chronic and will thus likely require lifelong therapies that begin at a young age. The screen was performed by Dr. Alan Mears in a normal human fibroblast (NHF) primary cell line. Confluent plates were dosed with a cocktail of five drugs for 8 hours, each at a standard concentration of 2 μM. An algorithm was used to sort the drugs into pools of 5 such that every drug appeared in the screen twice and no two drugs appeared in the same pool twice. The purpose of this was to avoid misinterpreting the effects of some compounds due to synergistic or antagonistic effects within the pool. Next, RNA was extracted from the harvested cells and quantitative real-time polymerase chain reaction (qPCR) was used to determine gene expression levels for 50 selected C4R genes compared to dimethylsulfoxide (DMSO) controls.

If substantial induction of any gene was seen in a pool, the experiment was repeated a second time in a different fibroblast primary cell line. If the results were reproducible, the pool was split up so that the response to each drug could be observed independently. One such pool, pool #20, showed a 4-fold upregulation of *SMAD3*. Upon separating the drugs from the pool, it became apparent that drug #592 (Isotretinoin) was responsible for the *SMAD3* induction (Figure 5).

13-cis-Retinoic Acid

13-cis-retinoic acid (13-CRA, generic name Isotretinoin) is a retinoid marketed under the brand name Accutane. It was first approved by the FDA for the treatment of severe acne in 1982[50]. Since this time, a wide range of therapeutic indications have emerged, including treatment of harlequin-type ichthyosis (a lethal skin disorder)[51] and chemopreventive treatments for several forms of cancer due to its influence on cell cycle progression[52-55]. Although 13-CRA is a potent teratogen[56, 57], it is safe for long-term use in males and non-pregnant females making it an attractive candidate for chronic disease therapy. Due to its widely recognized benefits, the pharmacokinetics of 13-CRA have been studied extensively in both humans and animals. There are large differences between its pharmacokinetic properties in mouse and human. In mice, the half-life ($t_{1/2}$) after an oral dose has been shown to be as long as 46 minutes[58], and as short as 19 minutes[59]. By contrast, pharmacokinetic studies in humans have found the $t_{1/2}$ to range from 4 hours[60] to as long as 167.4 hours[61]. According to BASF Chemical Company Canada and Roche Laboratories, the $t_{1/2}$ is between 17 and 21 hours[62, 63]. Oral therapeutic doses in humans generally range from 0.5-1 mg/kg daily for acne treatment[50], resulting in peak plasma levels of 300 and 860 ng/ml in fasted and fed

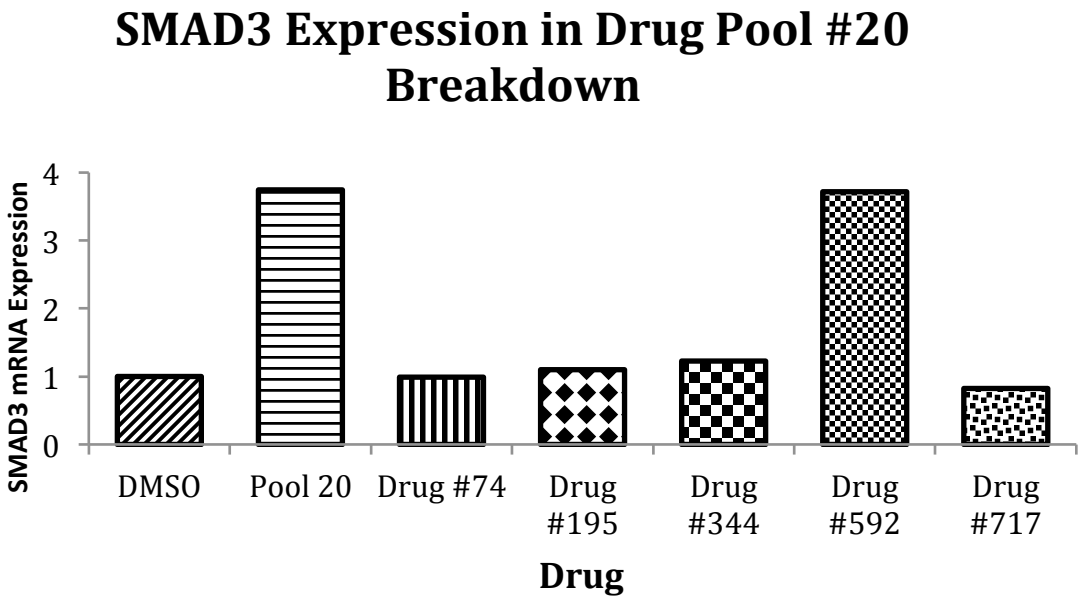

Figure 5. qPCR results for *SMAD3* expression in NHF dosed with various compounds. The induction seen in drug pool #20 appears to be due to drug #592 (Isotretinoin). Gene expression normalized to GAPDH and HPRT1. Two technical replicates were performed.
qPCR done by Dr. Alan Mears.

states, respectively[63]. No statistically significant differences in pharmacokinetics have been observed between pediatric and adult patients[63].

13-CRA is lipid-soluble and is 99.9% albumin-bound in serum. It is estimated that when taken orally the bioavailability is between 25% and 50%, and that this is maximized by consumption with a high-fat diet[62, 64]. Side effects are usually minor, the most common of which are dryness of skin, lips, eyes, and/or mouth. A small percentage of patients have reported headaches, fatigue, and joint pain, and in rare instances more severe side effects have been reported[65].

Retinoids and *SMAD3*

Retinoids exert their effects by binding to retinoic acid receptors (RARs) and retinoic X receptors (RXRs), each of which have α, β, and γ subtypes[66]. 13-CRA has five known metabolites: 4-*oxo*-retinoic acid (RA), all-*trans*-RA (tretinoin), all-*trans*-4-*oxo*-RA(4-*oxo*-tretinoin), 9-*cis*-RA and 9-*cis*-4-*oxo*-RA[50]. 4-*oxo*-RA is the major metabolite and has been shown to predominate over 13-CRA in serum concentration by a factor of about 4[61, 63, 67]. Of these metabolites, two are biologically important: only tretinoin and 9-cis-RA are able to bind RARs with high affinity, and only 9-cis-RA is able to bind RXRs[68]. When RAR and RXR bind their ligands, they heterodimerize and enter the nucleus where they interact with retinoic acid response elements (RAREs) in promoters of target genes. It is thought that each of the receptor subtypes is responsible for affecting distinct gene expression patterns related to cell growth and differentiation[66]. Neither human nor mouse *SMAD3* promoters contain any known RAREs (Figure 6), making direct interaction between 13-CRA and *SMAD3* unlikely.

A

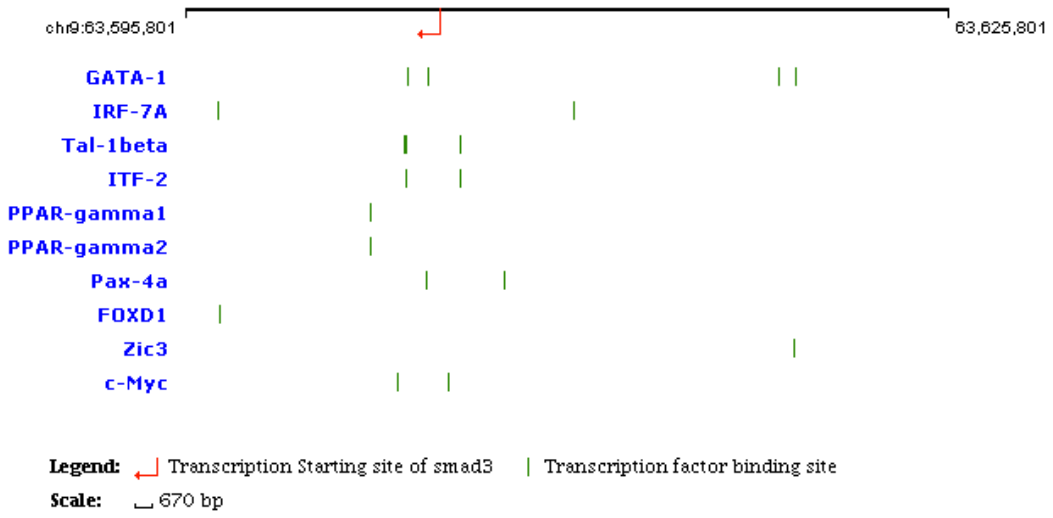

B

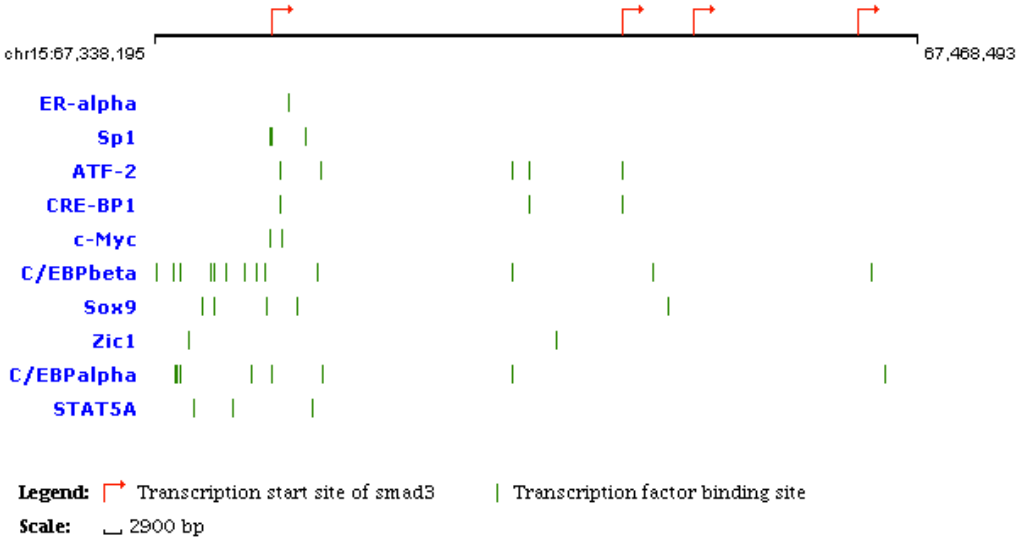

Figure 6. 10 most-relevant transcription factors in (A) mouse and (B) human *SMAD3* promoter. Note the lack of RARE in both. Images and complete list of transcription factors can be found at http://www.sabiosciences.com/chipqpcrsearch.php?app=TFBS.

Our lab has consistently seen 13-CRA-induced *SMAD3* induction in a variety of cell lines and is not the first to report this relationship[49, 69-72]. Given the potential to treat haploinsufficient disorders by manipulating the remaining functional WT allele[73, 74], use of 13-CRA to overexpress WT *SMAD3* may be beneficial to AOS patients. The limited treatment options for this fatal disorder underline the need for an effective therapy. Herein we provide evidence of *SMAD3* induction by 13-CRA *in vitro*, followed by a brief investigation of the mechanism of induction. Taken together our results provide a foundation to move forward with investigation of 13-CRA as a potential treatment for AOS.

MATERIALS AND METHODS

Cell Lines

All cell lines were grown in Dulbecco's Modified Eagle's Medium (DMEM) supplemented with 1% (v/v) L-glutamine. Media for NHF cells and patient fibroblasts was supplemented with 10% (v/v) fetal calf serum (FCS) (Sigma, F1051) while both VSMC lines were supplemented with 20% FCS. All cell lines were supplemented with 1% penicillin/streptomycin (v/v) (HyClone, SV30010) and grown at 37°C in a 5% CO_2 atmosphere. Culture media was changed 2-3 times per week and cells were passaged 1:2, 1:3, or 1:4 when required.

Drug Dosing

For all cell lines, media was changed directly before drug dosing. Cells were 90-100% confluent at time of dosing. 13-CRA (Sigma, #R3255) was diluted in DMSO. Dosing volume was 0.1% of media volume. When harvesting, cell pellets were split 4:1 for protein and RNA processing, respectively.

RNA Extraction and cDNA Synthesis

Cells were trypsinized and cell pellets were stored at -80°C for no more than one week before processing. Cells were then lysed and total RNA was extracted using an RNeasy Micro Kit (QIAGEN, #74004) according to the manufacturer's instructions and quantified spectrophotometrically using a NanoDrop Spectrophotometer ND-1000. Total RNA was DNase-treated prior to RNA isolation using the DNase provided in the RNeasy

Micro Kit. cDNA was synthesized using iScript Advanced cDNA Synthesis Kit (BioRad, #172-5038) as per the manufacturer's instructions.

Quantitative Real-Time PCR

GAPDH and HPRT1 were used as reference genes in all qPCR experiments. *SMAD3* human primers detected all transcripts and were of forward sequence AGTGGAGCTGACACGGAGAC and reverse sequence CATCTGGGTGAGGACCTTGT. Smad3 mouse primers detected all transcripts and were of forward sequence GTTCTCCAAACCTCTCCCCG and reverse sequence CTCTCCCAATGTGTCGCCTT. qPCR was performed on a CFX96 Touch Real-Time PCR Detection System (BioRad #185-5195). Reactions were assembled using iQ SYBR Green Supermix (BioRad, #170-8882) to a total reaction volume of 20 ul. Primer concentrations were used at 10 μM. Data were analyzed using Bio-Rad CFX Manager 3.0 software.

Protein Extraction

Cells were trypsinized and cell pellets were stored at -80°C for no more than one week before processing. Cells were lysed using RIPA buffer supplemented with protease and phosphatase inhibitors. Samples were then sonicated for 30 seconds followed by a resting period of 30 seconds, repeated for a total of 8 minutes using a water bath sonicator (DiaMed Transsonic T460). Samples were then centrifuged at 4°C for 40 minutes. Protein was aspirated off and quantified using a Bradford Protein Assay (Bio-Rad #500-0006). Samples were prepared for Western blot using 4x Protein Loading

Buffer (Licor, #928-40004).

Immunoblotting

Protein extracts were harvested from confluent cells as described. 40 μg of protein was loaded on 11% acrylamide gels and run at 80 V for 30 minutes, then 120 V for 1 hour. The proteins were then transferred using a Semi-Dry transfer system (Amersham Biosciences TE 77 Semi-Dry Transfer Unit) onto nitrocellulose membrane (Bio-Rad, #162-0115) for 1 hour 15 minutes at 65 milliAmps/gel. Ponceau stain was used to detect total protein. Membranes were blocked in PBS/Tween (0.05% Tween-20) with 5% dried skimmed milk for 1 hour. Anti-SMAD3 antibody (Abcam #ab40854) was used at 1:3000 in PBS/Tween (0.05% Tween-20) with 5% dried skimmed milk powder overnight at 4°C. The secondary antibody was anti-rabbit and was used at 1:5000 (Cell Signaling Technology, #7074S) in PBS/Tween (0.05% Tween-20) with 5% dried skimmed milk powder at room temperature for 1 hour. Both primary and secondary antibody washes were followed by three 15-minute washes with PBS/Tween (0.05% Tween-20). Antigen detection was carried out using Clarity (Bio-Rad, #170-5061) according to the manufacturer's instructions. Loading control anti-HSC70 (Santa Cruz Biotechnology, #sc-7298) was used at a concentration of 1:2000 in PBS/Tween (0.05% Tween-20) with 5% dried skimmed milk powder at room temperature for 1 hour. The secondary antibody, anti-mouse, was used at 1:5000 (Cell Signaling Technology, #7076S) in PBS/Tween (0.05% Tween-20) with 5% dried skimmed milk powder at room temperature for 1 hour. All images were quantified using ImageJ 1.48v software.

Immunostaining

For immunofluorescence detection, cells were fixed with 4% PFA in PBS for 10 minutes and incubated with SMAD3 primary antibody (1:100; Abcam #ab40854) diluted in PBS/Triton X-100 for 1 hour. Secondary antibody was Alexa 488 (1:750, Life Technologies #A11008) diluted in PBS/Triton X-100 for 1 hour. Cells were counterstained with DAPI. Coverslips were mounted with Vectashield H-1000 (Vector Laboratories).

Statistical Analysis

Experimental data were analyzed using GraphPad Prism (v5.0c). Statistical analysis was performed using one-way ANOVA and post hoc analysis was Tukey's test. *P* values <0.05 were considered significant and are marked with asterisks in bar graphs. ** $p<0.005$, and ***$p<0.001$. All error bars are expressed as standard error of the mean (SEM) as indicated.

RESULTS

13-cis-retinoic acid induces *SMAD3* in NHF and patient cell lines

We used WT and patient (*SMAD3*+/-) primary fibroblast cell lines to verify a positive result from a broad scale FDA drug screen performed in our laboratory. 13-CRA concentrations of 100, 200, and 500 nM were used to mimic therapeutic serum levels. Statistically significant upregulation of *SMAD3* RNA was seen in NHF at 8 hours for 200 and 500 nM concentrations of 13-CRA, with the higher concentration having a more significant response (Figure 7). While a trend towards protein induction was seen at 8 hours, statistically significant induction was not observed (Figure 8). At 16 hours, RNA induction was significant at a concentration of 500 nM 13-CRA only (Figure 9), and protein induction was increased 2.5 fold with statistical significance at 200 and 500 nM concentrations (Figure 10).

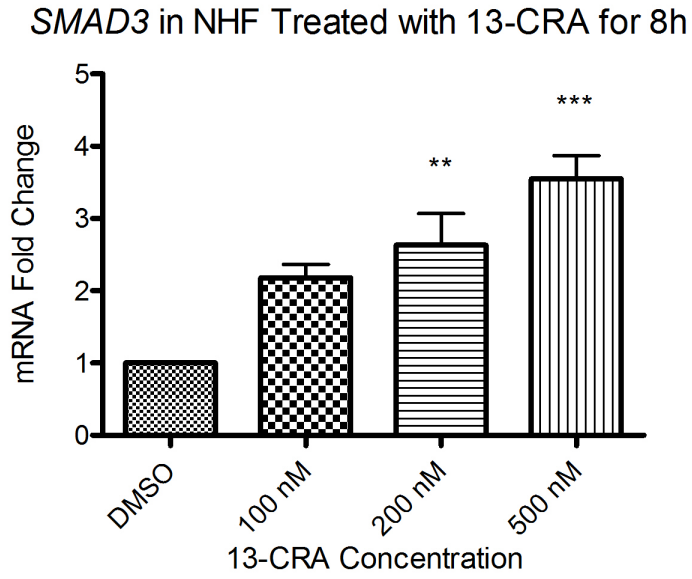

Figure 7. *SMAD3* RNA expression in NHF dosed with various concentrations of 13-CRA for 8 hours. Error bars represent SEM. n=4.

*p < 0.05
** p < 0.01
*** p < 0.001

A

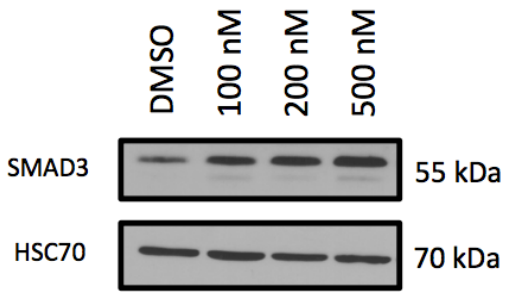

B

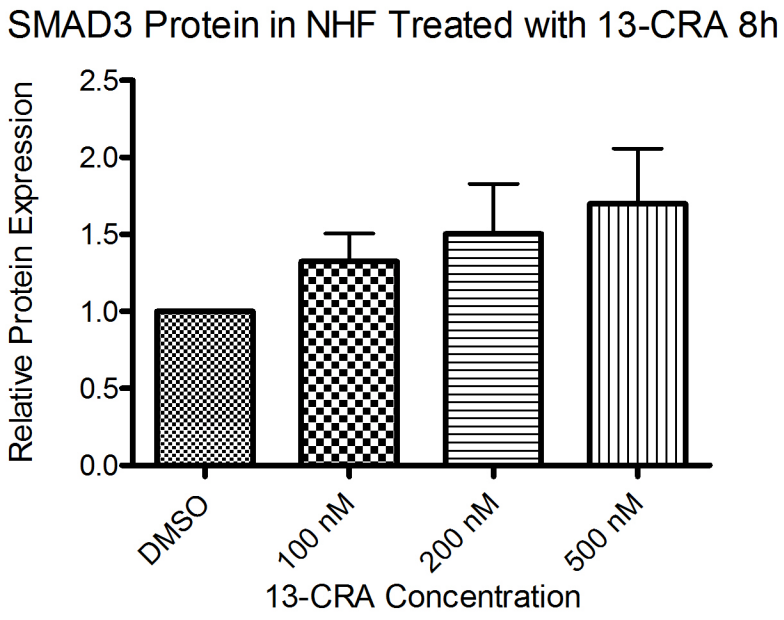

Figure 8. A) Sample Western blot for SMAD3 protein in NHF treated with various concentrations of 13-CRA for 8 hours. B) Quantified SMAD3 protein expression. Error bars represent SEM. N=4.

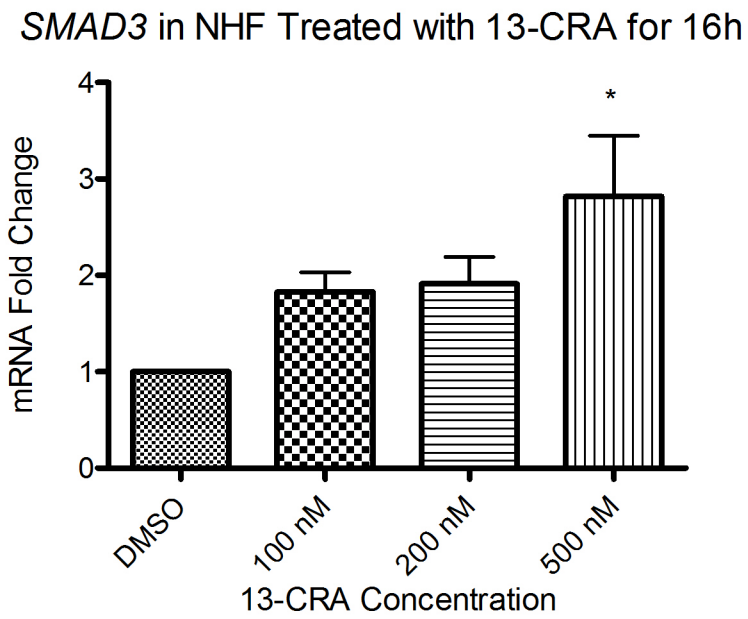

Figure 9. *SMAD3* RNA in NHF dosed with various concentrations of 13-CRA for 16 hours. Error bars represent SEM. N=4.

*$p < 0.05$

A

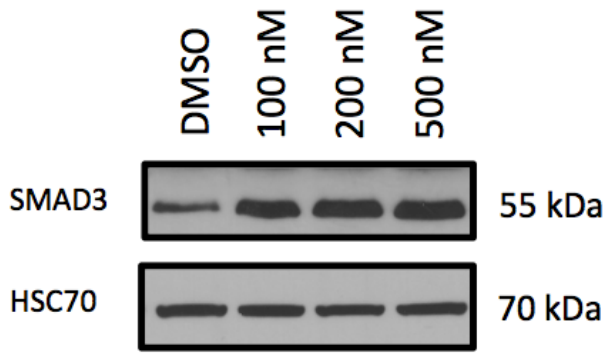

B

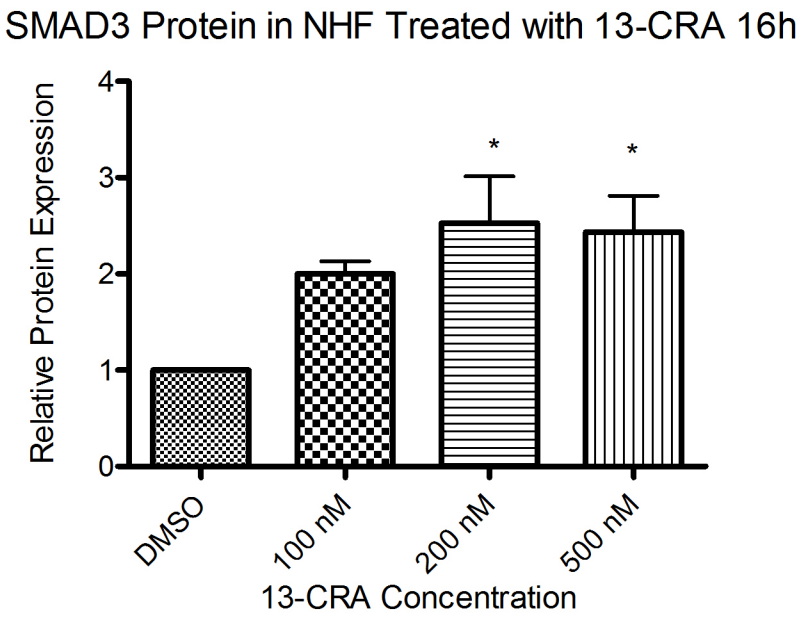

Figure 10. A) Sample Western blot for SMAD3 protein in NHF treated with various concentrations of 13-CRA for 16 hours. B) Quantified SMAD3 protein expression. Error bars represent SEM. n=4.

*$p < 0.05$

Next, we obtained fibroblasts from a 65-year old female with AOS. The patient has a family history of aortic aneurysm secondary to a mutation of *SMAD3*. The mutation is a 40 kb deletion that encompasses exon 4 to the end of the gene. Patient findings include arthritis, bifid uvula, and mitral valve prolapse with mitral regurgitation. The patient takes no medication other than Zantac for Fundic gland polyps of minimal clinical significance. Due to a lack of serious symptoms, the patient was only diagnosed with AOS at the age of 65 after self-referral for diagnostic purposes based on family history and concerns for her children.

qPCR for *SMAD3* transcripts showed that the patient cells contain approximately half the *SMAD3* RNA of the WT cells. Furthermore, the patient cells responded well to a 500 nM concentration of 13-CRA, which nearly doubled *SMAD3* transcripts in both cell lines (Figure 11A) after 8 hours. Western blots confirmed that patient cells contained approximately half the SMAD3 protein of NHF (Figure 11B). We repeated the same set of 13-CRA treatments on the patient cells at time points of 8, 16, and 24 hours. Significant RNA induction was seen at 8 hours, but not 16 or 24 hours (Figure 12 A, B, C). SMAD3 protein levels showed a modest trend of induction at 8 and 24 hours, but only achieved significance at 16 hours for a 200 nM concentration (Figure 13 A, B, C). A time course of this induction at each concentration is shown in Figure 14.

As SMAD3 must become activated and enter the nucleus to exert its transcriptional effects, we sought to see whether the additional SMAD3 protein was localizing appropriately. Immuofluorescent imaging with anti-SMAD3 antibody showed increasing protein in the nucleus of patient cells corresponding to increasing

concentrations of 13-CRA, as indicated by DAPI staining (Figure 15). SMAD3 protein was also visible in the cytoplasm to a much lesser extent (Appendix A).

A

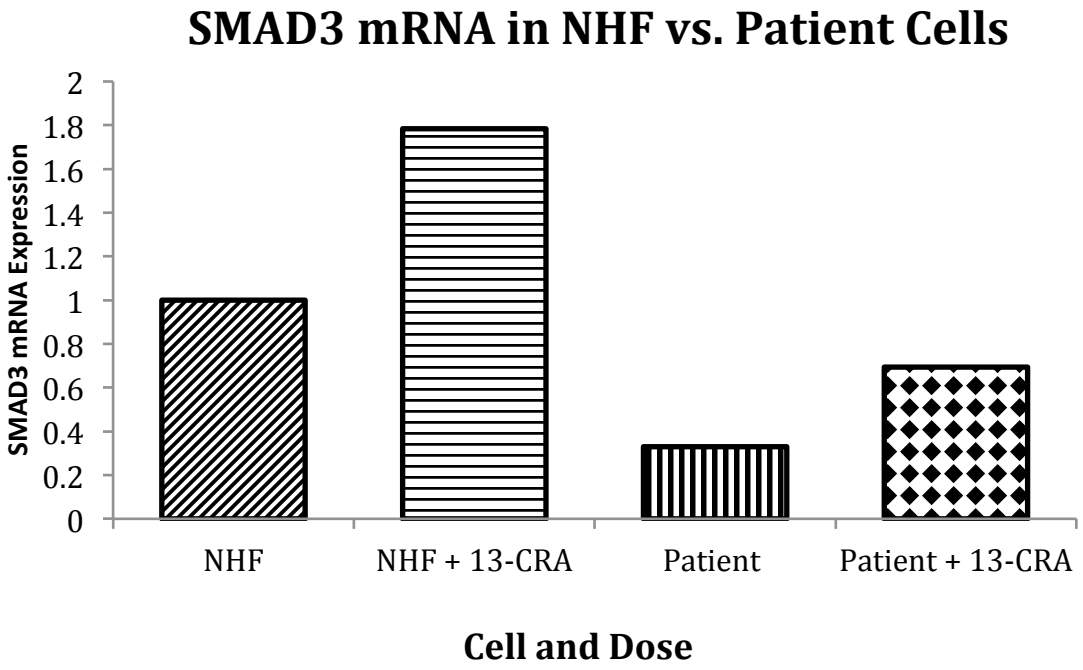

B

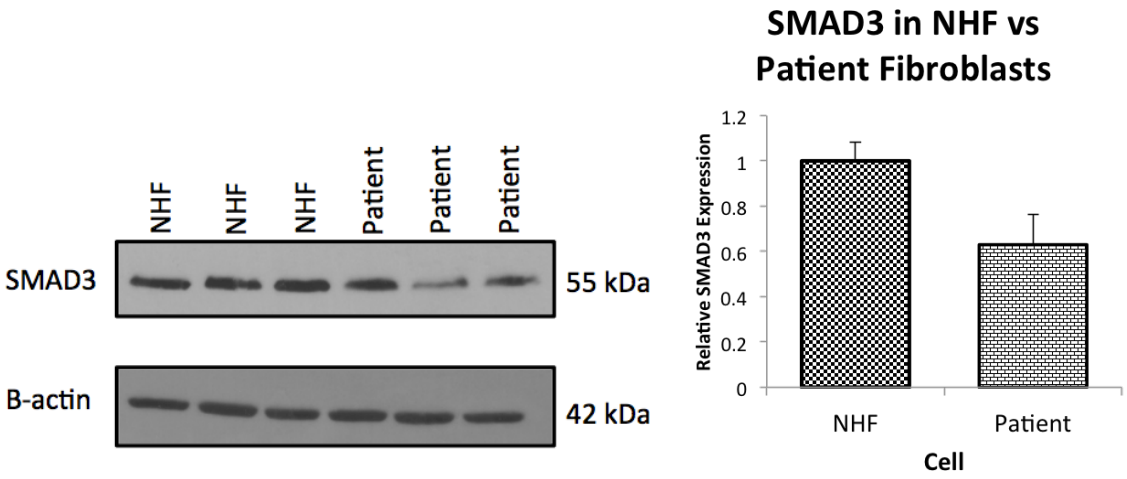

Figure 11. Endogenous *SMAD3* is reduced in patient cells. A) SMAD3 transcripts in NHF and patient fibroblasts dosed with 500 nM 13-CRA for 8 hours. Two technical replicates were performed. qPCR by Dr. Alan Mears.
B) Western blot and quantification comparing SMAD3 protein in NHF and AOS patient fibroblasts.

A

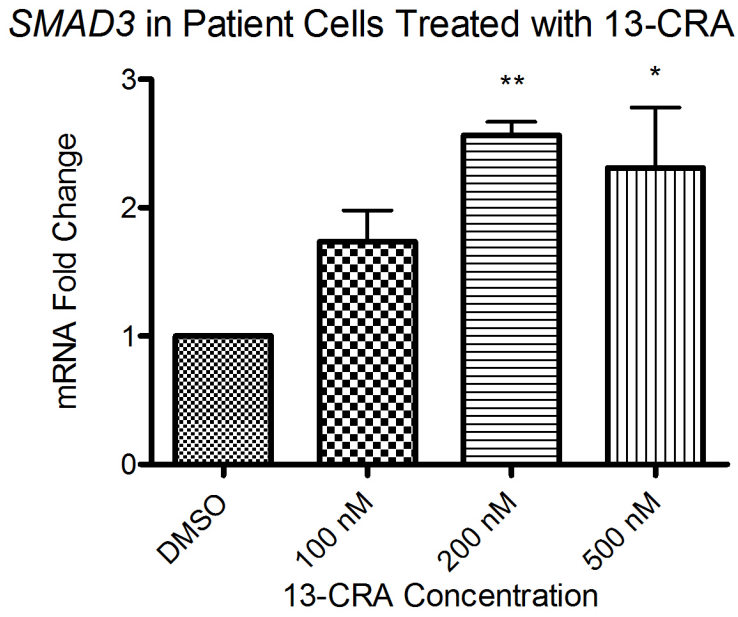
SMAD3 in Patient Cells Treated with 13-CRA for 8h
mRNA Fold Change
3
2
1
0
**
*
DMSO
100 nM
200 nM
500 nM
13-CRA Concentration

B

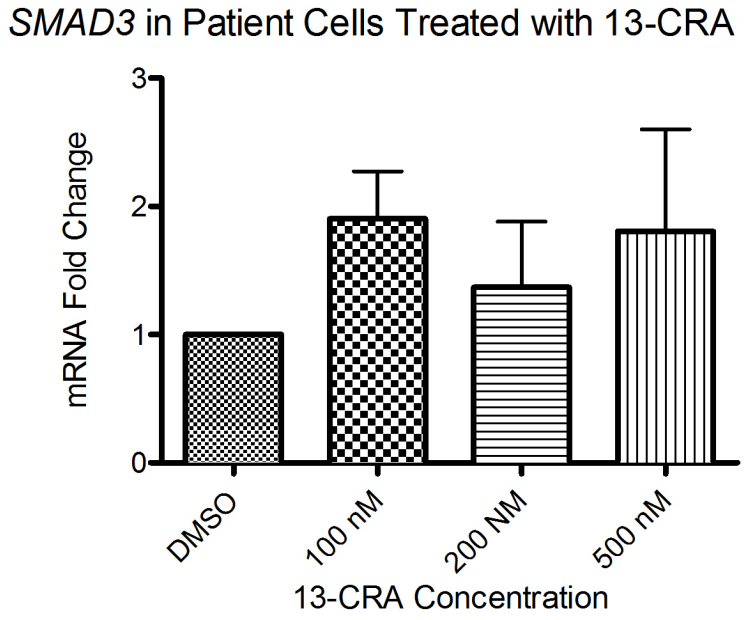
SMAD3 in Patient Cells Treated with 13-CRA for 16h
mRNA Fold Change
3
2
1
0
DMSO
100 nM
200 NM
500 nM
13-CRA Concentration

C

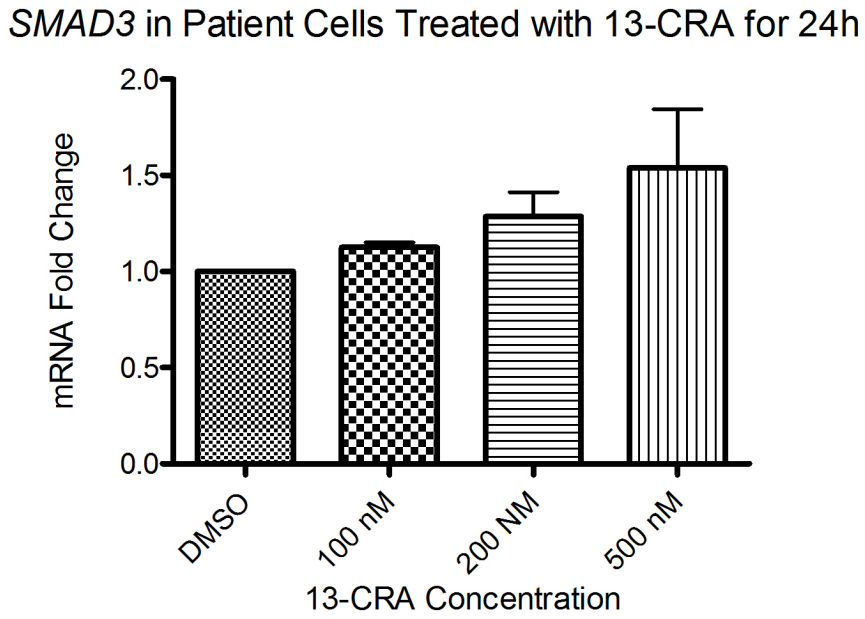

Figure 12. *SMAD3* RNA in patient fibroblasts dosed with various concentrations of 13-CRA for A) 8, B) 16, and C) 24 hours. Error bars represent SEM. n=4.

*p < 0.05

** p < 0.01

A

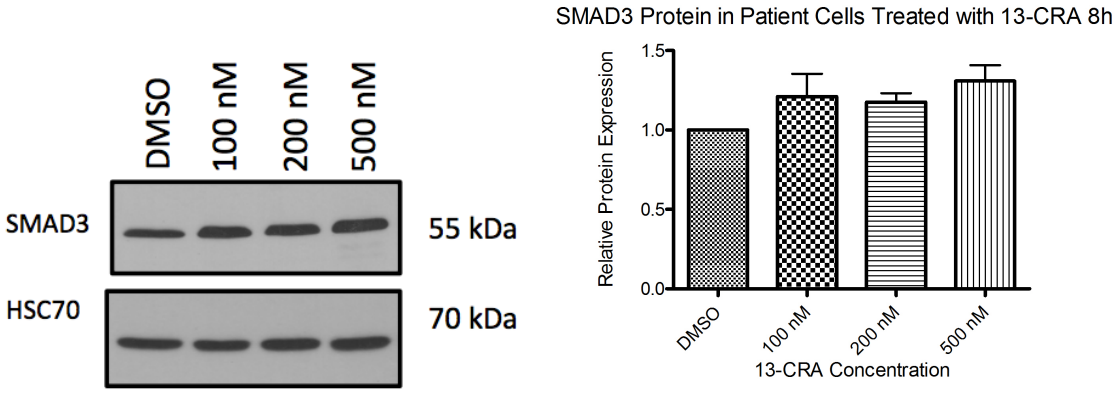

B

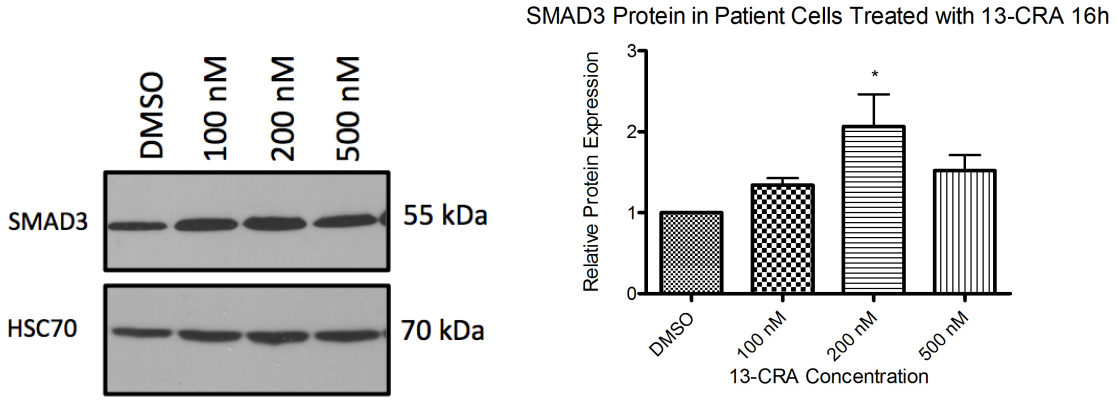

C

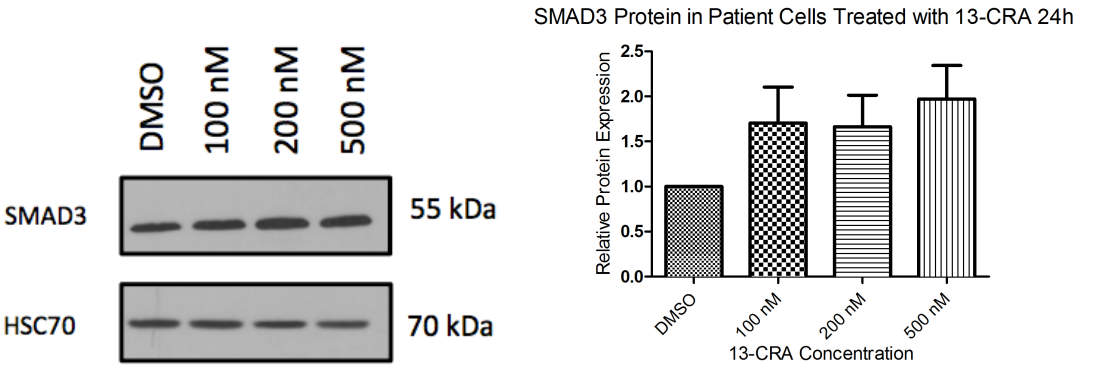

Figure 13. Western blot for SMAD3 protein in patient cells treated with various concentrations of 13-CRA for A) 8, B) 16, and C) 24 hours. n=4 for each panel.
*$p < 0.05$

A

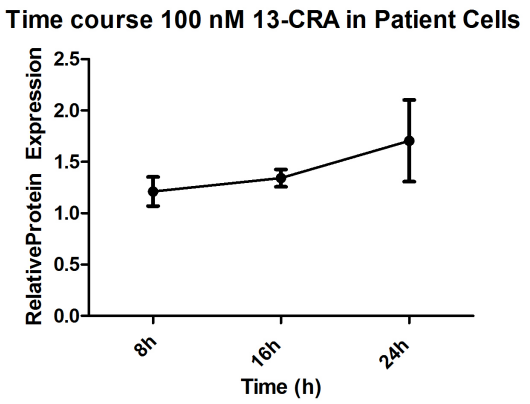

B

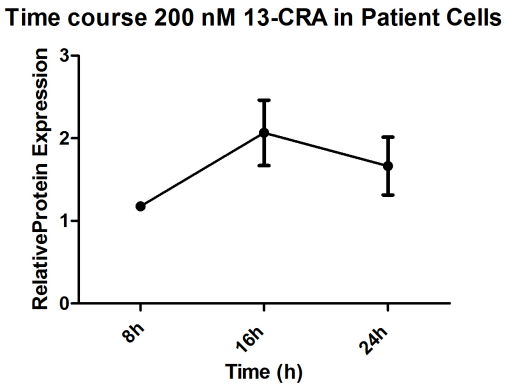

C

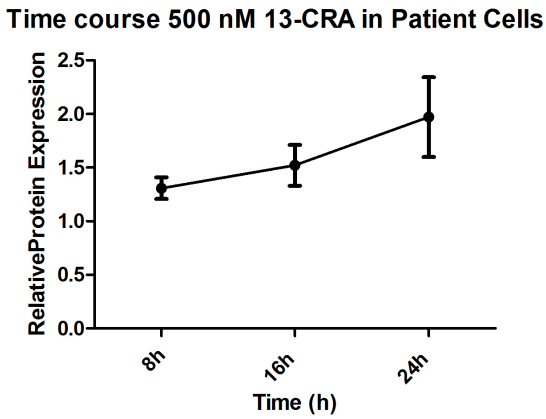

Figure 14. SMAD3 protein induction time course for A) 100, B) 200, and C) 500 nM treatments with 13-CRA. Error bars represent SEM. n=4.

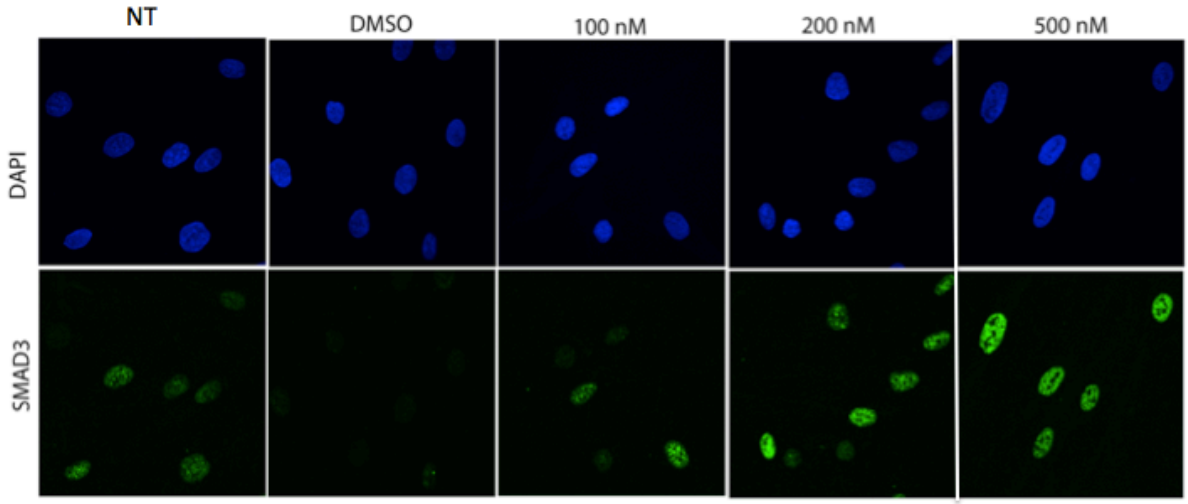

Figure 15. Immunofluorescent images of nuclear SMAD3 in patient cells at various concentrations of 13-CRA after 8 hours. Nuclei are counterstained with DAPI. NT = not treated.

Induction in mouse VSMCs

Because AOS primarily affects the aorta, the *Smad3* expression of aortic VSMCs is of particular interest. We obtained VSMCs from the aortas of WT and AOS mice and ran parallel experiments in these lines, called WT5 and S7, respectively. We repeated the previous experiments using 100, 200, and 500 nM concentrations of 13-CRA. RNA response in treated S7 cells was highly variable and showed a non-significant trend towards induction at 8 hours (Figure 16). By contrast, Western blots showed no SMAD3 protein induction in the S7 cells at 8 hours (Figure 17A, B). A 16 hour treatment on S7 cells did not evoke a significant response in *Smad3* transcription (Figure 18), and protein levels remained unchanged (Figure 19A, B). In WT5 VSMCs, a non-significant induction of *Smad3* RNA was evoked by 8 hour treatment (Figure 20), and a modest but statistically significant upregulation of protein was seen at this time point (Figure 21A, B). At 16 hours, significant RNA induction was seen (Figure 22), but not protein (Figure 23A, B).

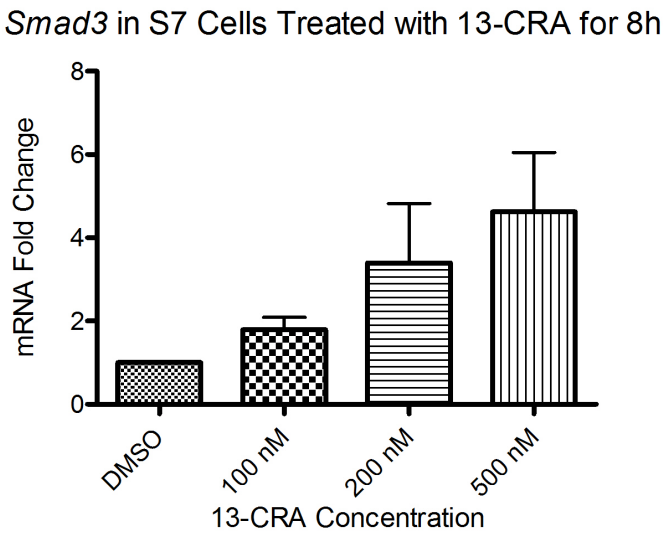

Figure 16. *Smad3* RNA in S7 cells dosed with various concentrations of 13-CRA for 8 hours. Error bars represent SEM. n=4.

A

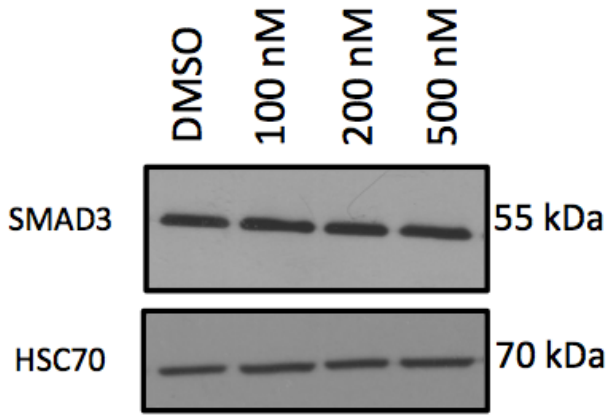

B

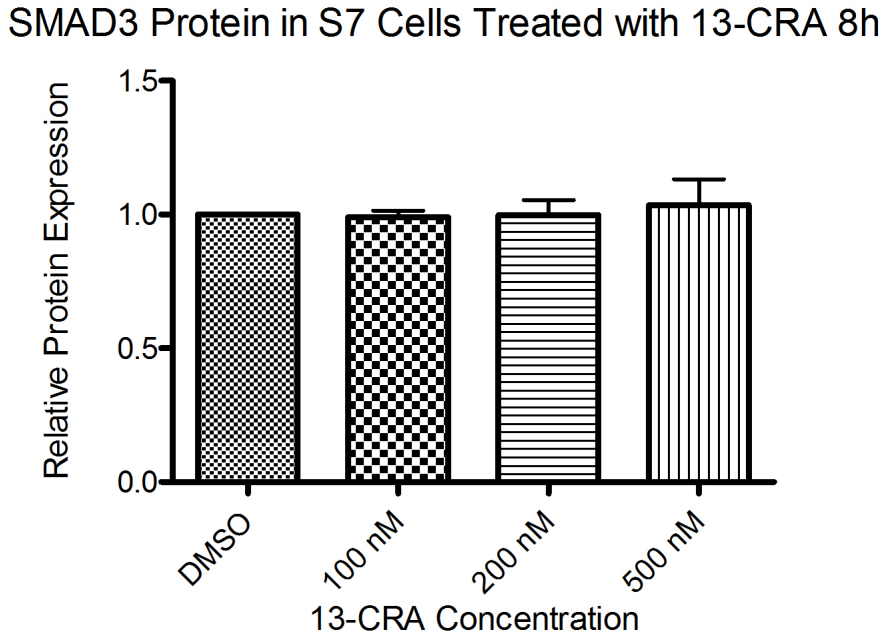

Figure 17. A) Sample Western blot for SMAD3 protein in S7 cells treated with various concentrations of 13-CRA for 8 hours. B) Quantified SMAD3 protein expression. Error bars represent SEM. n=4.

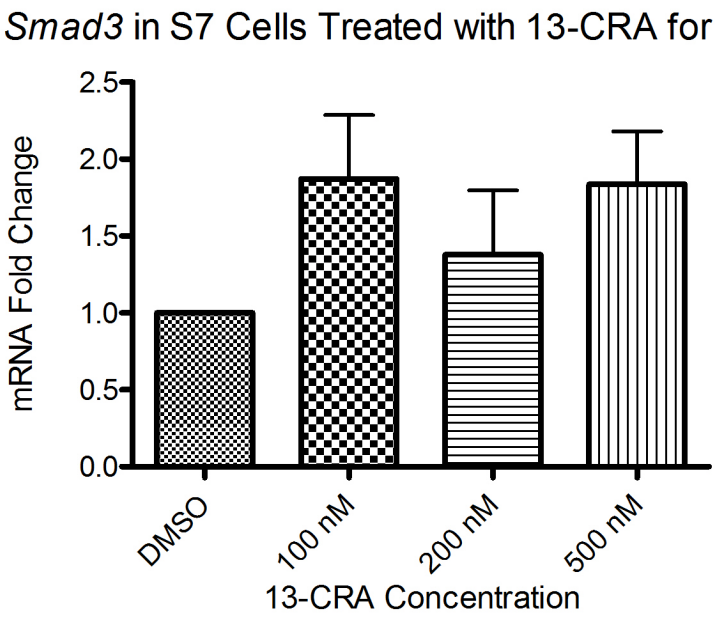

Figure 18. *Smad3* RNA in S7 cells dosed with various concentrations of 13-CRA for 8 hours. Error bars represent SEM. n=4.

*p < 0.05
** p < 0.01
*** p < 0.001

A

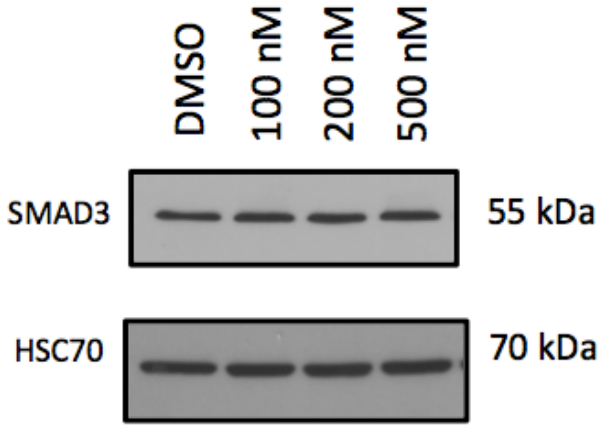

B

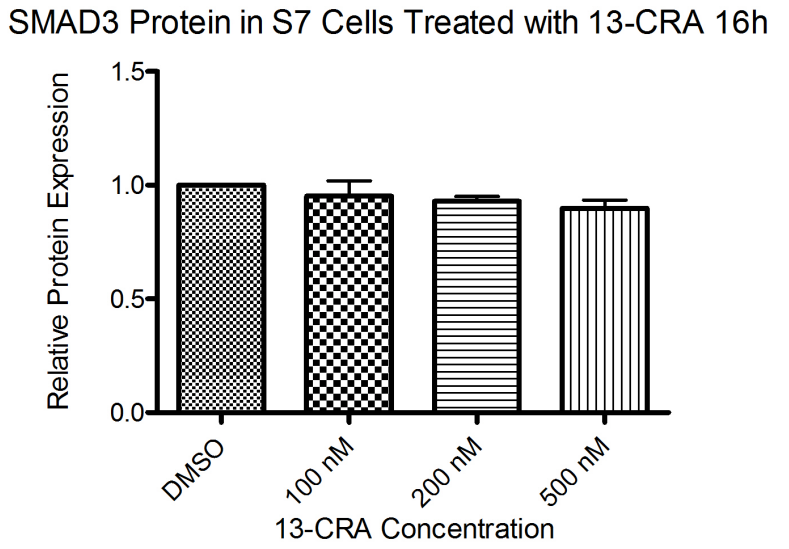

Figure 19. A) Sample Western blot for SMAD3 protein in S7 cells treated with various concentrations of 13-CRA for 16 hours. B) Quantified SMAD3 protein expression. Error bars represent SEM. n=4.

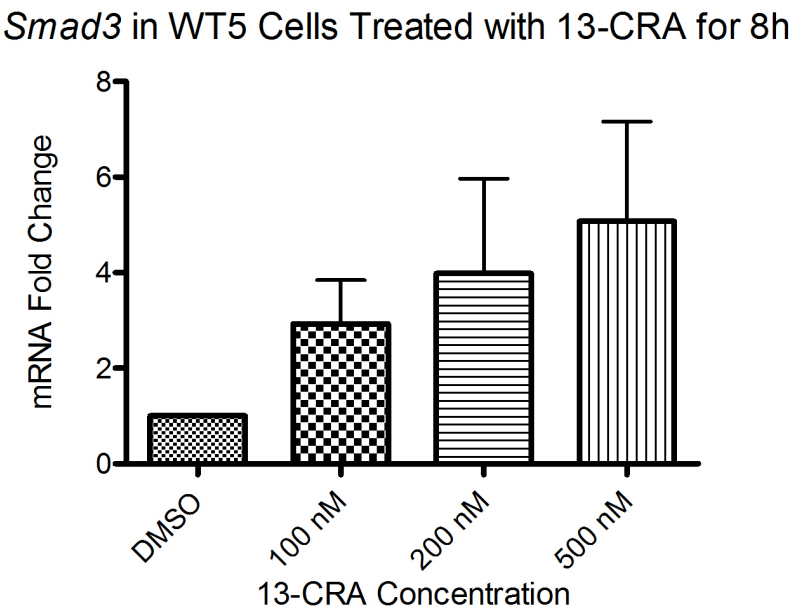

Figure 20. *Smad3* RNA in WT5 cells dosed with various concentrations of 13-CRA for 8 hours. Error bars represent SEM. n=4.

A

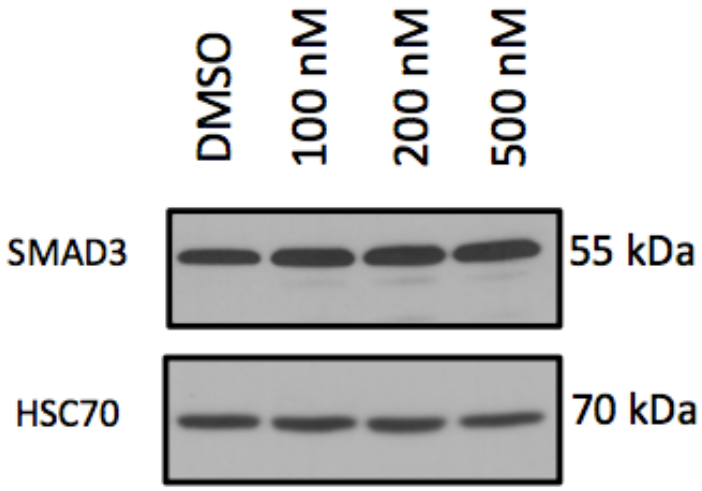

B

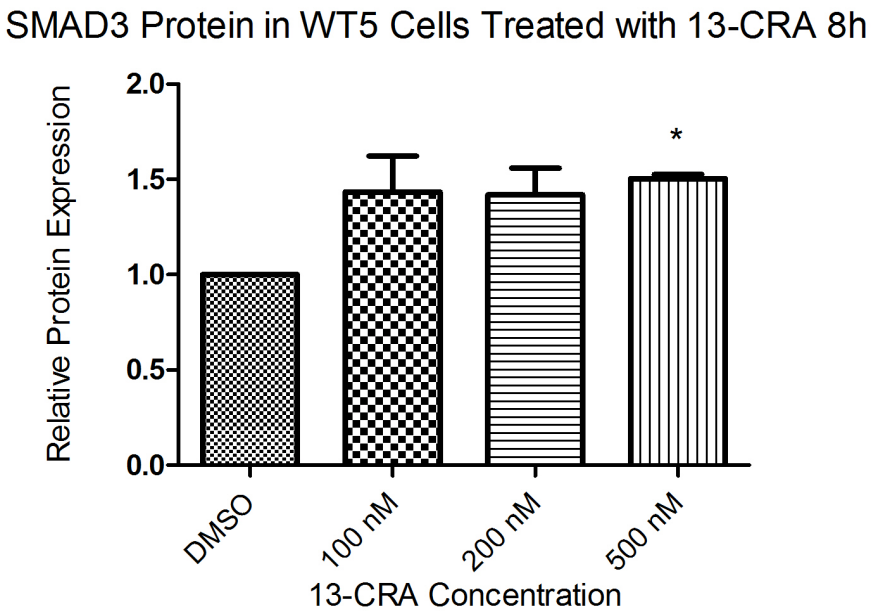

Figure 21. A) Sample Western blot for SMAD3 protein in WT5 cells treated with various concentrations of 13-CRA for 8 hours. B) Quantified SMAD3 protein expression. Error bars represent SEM. n=4.

*$p < 0.05$

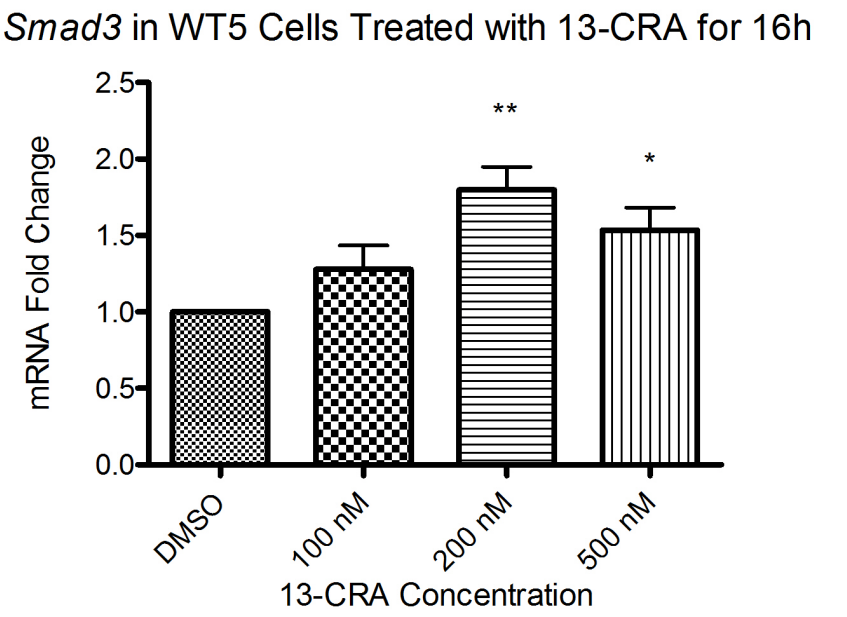

Figure 22. *Smad3* RNA in WT5 cells dosed with various concentrations of 13-CRA for 16 hours. Error bars represent SEM. n=4.

*p < 0.05

** p < 0.01

A

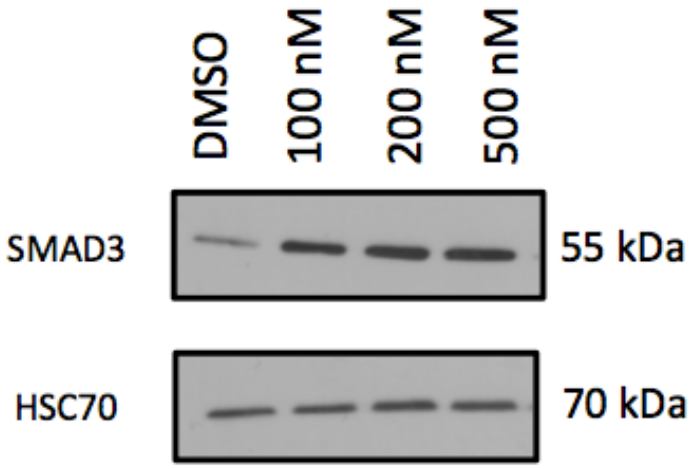

B

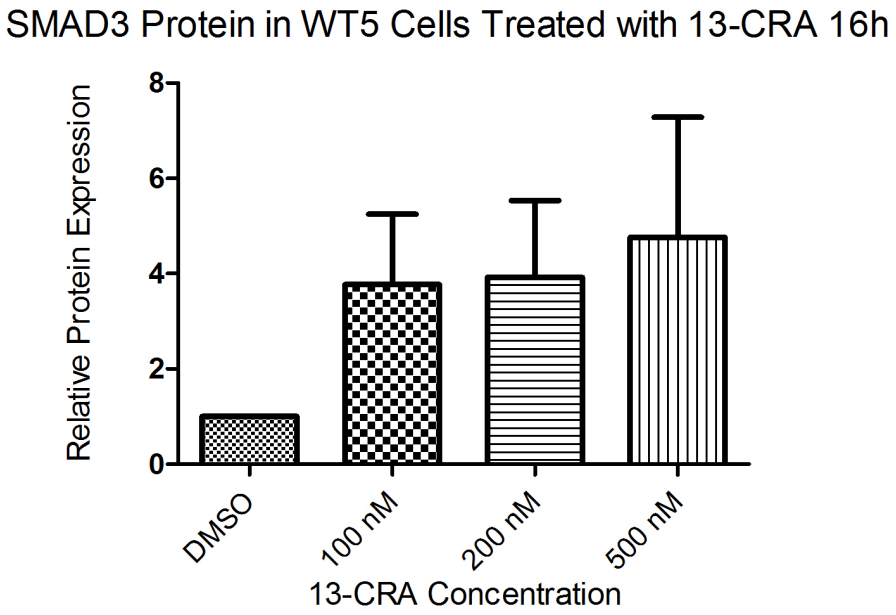

Figure 23. A) Sample Western blot for SMAD3 protein in WT5 cells treated with various concentrations of 13-CRA for 16 hours. B) Quantified SMAD3 protein expression. Error bars represent SEM. n=4.

C/EBPβ may play a role in *SMAD3* induction

We noted that the human *SMAD3* promoter contains several transcription factor binding sites for CCAAT-enhancer-binding protein β (C/EBPβ), and thus thought it a good candidate for investigation as a protein intermediate. To see if C/EBPβ plays a role in *SMAD3* induction, we dosed NHF with 200 nM 13-CRA in combination with increasing concentrations of the C/EBPβ inhibitor N-acetyl-D-sphingosine. At 60 uM of the inhibitor, *SMAD3* induction was blocked; both transcript and protein levels were comparable to NHF dosed with DMSO control (Figure 24A, B).

A

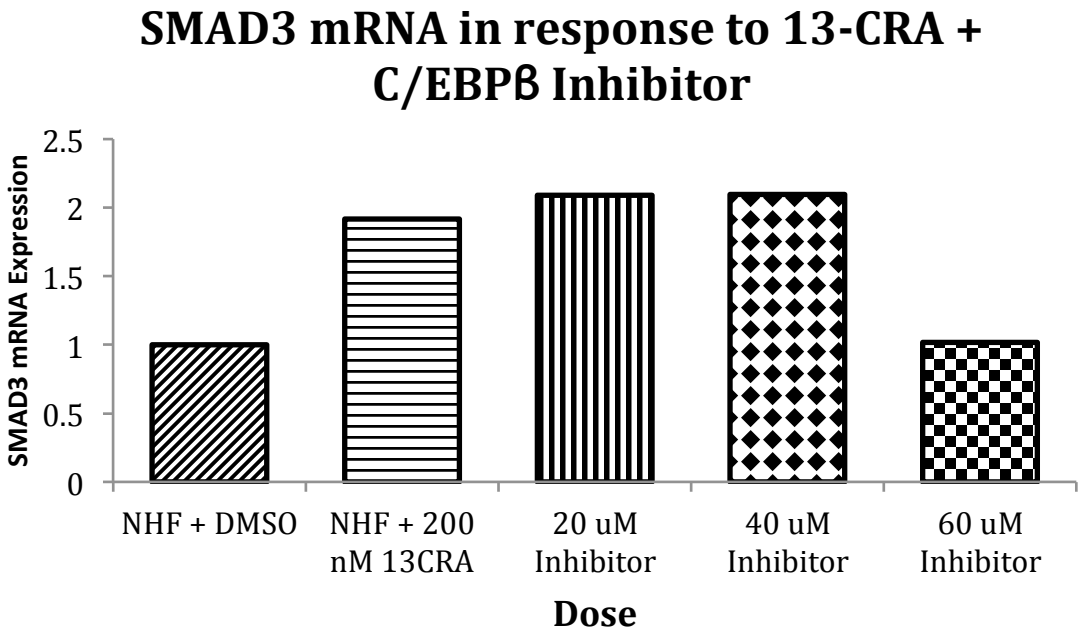
SMAD3 mRNA in response to 13-CRA + C/EBPβ Inhibitor
SMAD3 mRNA Expression
2.5
2
1.5
1
0.5
0
NHF + DMSO
NHF + 200 nM 13CRA
20 uM Inhibitor
40 uM Inhibitor
60 uM Inhibitor
Dose

B

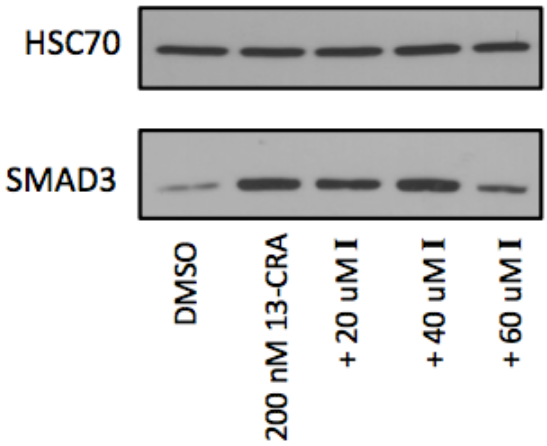

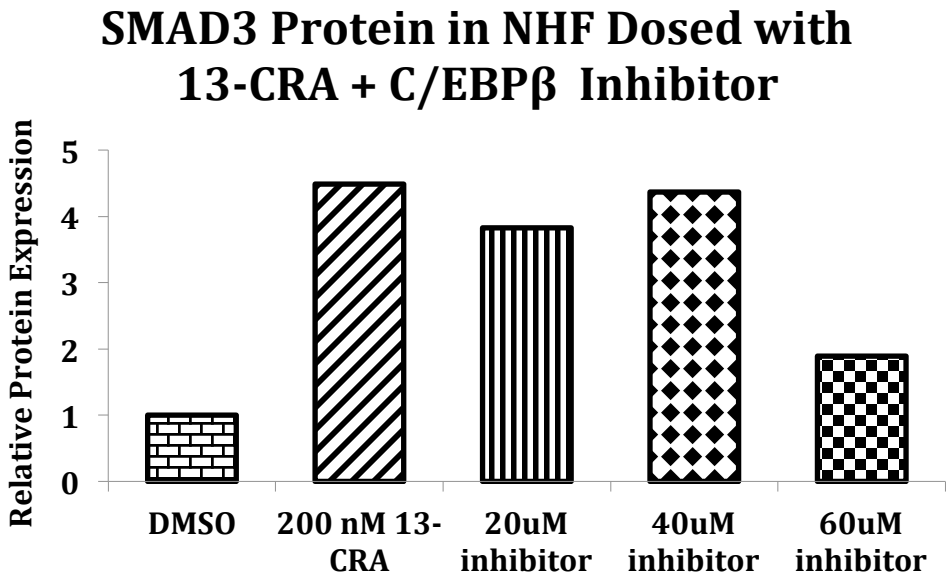

Figure 24. A) *SMAD3* RNA response in NHF to 200 nM 13-CRA in combination with increasing concentrations of C/EBPβ inhibitor N-acetyl-D-sphingosine. 2 technical replicates were performed. qPCR by Dr. Alan Mears. B) Western blot and quantification for SMAD3 protein in NHF dosed with 200uM 13-CRA in combination with increasing concentrations of C/EBPβ inhibitor.

DISCUSSION

AOS is one of approximately 7000 rare diseases that impose significant burden on patients, families, and the health care system. Due to a lack of external symptoms this devastating disorder often goes undiagnosed until a fatal aortic rupture occurs, and several cases likely go undiagnosed even after such a rupture. Unfortunately, even if detected, treatment options are limited to monitoring the major arteries for distension and invasive surgery to intervene before rupture occurs. Thus, there is a need for the development of a therapy that halts disease progression and possibly repairs vessel damage. In this report, we demonstrate that a chemical treatment modality can increase expression of *SMAD3 in vitro,* which consequently may be able to prevent and even reverse aneurysm development in AOS patients.

Results

In this report, we investigated the effects of 100, 200, and 500 nM concentrations of 13-CRA on RNA and protein in NHFs, patient fibroblasts, and mouse VSMCs. Our results show considerable variability, particularly in mouse cultures. In NHFs, we saw statistically significant induction of *SMAD3* RNA at 8 hours post-dosing at concentrations of 200 and 500 nM 13-CRA, and at 16 hours post-dosing for the 500 nM concentration. While there was a trend towards protein induction at 8 hours, we only observed a statistically significant increase at 16 hours for 200 and 500 nM concentrations; this data suggests a lag time between transcription and translation. Although not statistically significant, the 500 nM concentration of 13-CRA invoked a 1.7-fold mean increase in SMAD3 protein at 8 hours. In haploinsufficiency disorders

cells theoretically produce 50% of the protein present in WT cells, which is not enough for regular function. However, small changes in the levels of some proteins can have profound biological significance and be enough to reinstate proper function. Because of this, even a 1.7-fold increase in SMAD3 protein may be enough to improve AOS disease phenotype.

In patient fibroblasts, we showed that *SMAD3* RNA and protein was approximately half that in NHFs. Moreover, we showed that both cell lines responded to a 500 nM concentration of 13-CRA by nearly doubling *SMAD3* transcripts. We saw a significant increase in RNA induction at 8 hours post-dosing at 200 and 500 nM concentrations of 13-CRA. This was not reflected in protein levels at that time point, where no induction was seen. However, immunofluorescent images of SMAD3 protein in these cells did show a marked increase in nuclear SMAD3 corresponding to increasing concentrations of 13-CRA. Such a stark image was surprising given the lack of protein induction depicted by Western blot. One reason for this could be the relatively small size of the nucleus compared to the whole cell volume. As whole cell lysates were used for protein processing, an increase in nuclear SMAD3 may have been obscured by a relatively unchanged concentration of SMAD3 in the larger cytoplasmic portion. Isolating nuclei prior to protein extraction for Western blot, or using an antibody specific to phosphorylated (activated) SMAD3, may provide a more accurate picture. At a 16-hour time point in patient cells, RNA levels were largely variable between trials and did not exhibit a trend. At 24 hours, the 500 nM concentration had a non-significant mean RNA increase of 1.5 fold. Western blots showed a significant increase of SMAD3 protein

at 16 hours for a 200 nM concentration. At 24 hours, protein trended towards 1.5 fold induction, but again large variability between samples existed.

In VSMC lines, we saw highly variable results. In both WT and *Smad3*+/- VSMCs, we observed a non-significant 5-fold mean induction of *Smad3* RNA 8 hours post-dosing. This experiment was performed with a newly purchased batch of 13-CRA, thus we initially thought that the large dose response was indicative of degradation in our old 13-CRA aliquots. However, Western blots for both 8 and 16-hour time points in *Smad3*+/- VSMCs showed no change in protein levels. It is therefore unclear whether the trend seen was due to the use of fresh compound, or if the response in mouse cells is naturally greater than in human cells. We did observe significant SMAD3 protein induction in WT VSMCs at 8 hours post-dosing, and a non-significant 4-fold mean induction at 16 hours. We are currently unable to explain the discrepancy between the trend in RNA induction and lack of corresponding response in protein. While there are large differences in 13-CRA metabolism between mouse and human, these are most likely due to differences in liver enzymes that are not generally applicable to tissue culture. It is possible that protein induction in the *Smad3*+/- line was transient and had been degraded by 16 hours, or that additional doses are needed to maintain RNA induction long enough to be translated into protein. Further *in vitro* studies with additional time points and replicates are needed to elucidate mouse cell response.

Having seen results consistently trend towards induction, we do believe that there is a positive dose-response relationship between 13-CRA and *SMAD3*. There are several possible reasons for the observed variability. While all cells for each experiment were matched for passage number and confluence, it is possible that minute differences in cell

density had profound effects on 13-CRA metabolism. Other differences in microenvironment such as the position of plates in the incubator may have played a role as heat consistency or physical disturbances can stress cells and alter metabolism. Finally, both VSMC lines were quite unstable, which may be inherent to the cell lines or partially due to agitation during transportation from another institution. Increasing replicate size beyond n=4 may help decrease the size of error bars.

13-CRA and SMAD3

Ours is not the first study to report a relationship between *SMAD3* and retinoid molecules. The Broad Connectivity Map (CMAP 2.0) compound database, a genome-wide expression reference collection of cultured human cells' response to various compounds, reported increased *SMAD3* RNA expression in response to Isotretinoin[49]. A study by the Pennsylvania State University College of Medicine Department of Dermatology found that *SMAD3* expression was increased in immortalized sebocytes from patients treated with 13-CRA for severe acne (data accessible at NCBI GEO database[72], accession GSE10434). Both *in vitro* and *in vivo* Drug Matrix taxicogenomic studies have also observed increased *SMAD3* expression in hepatocytes of male Sprague-Dawley rats dosed with Isotretinoin[71]. In 2008, Xiao *et al*. found that in naïve $CD4^+$ T cells, RA induces *SMAD3* RNA as well as both phosphorylated and unphosphorylated SMAD3 protein[69]. Importantly, RA did not induce *SMAD2*, which is structurally similar yet functionally distinct from *SMAD3*, indicating that the induction is specific[69]. In adipocytes, RA has been reported to cause a robust induction of *SMAD3* RNA, with transcripts continuing to accumulate after 4 days of continuous RA treatment.

Protein induction was also seen in response to the same treatment, but the induction was transient and returned to baseline levels after 3 days of RA exposure[75]. Additional time course studies both *in vitro* and *in vivo* are needed to determine whether a similar trend exists in cell types relevant to AOS.

Pharmacologic modulation of haploinsufficient disorders

As with many genetic conditions, the broad biological consequences of mutations in the TGF-β/SMAD pathway and the resulting plethora of systemic, cognitive, and developmental consequences renders treating individual findings impractical, often impossible, and never curative. Other therapeutic options include providing exogenous mature protein. For delivery of intracellular proteins, gene therapy using adeno-associated virus is showing some progress[76], however it imposes significant costs and remains out of reach for most patients. Another experimental option is cDNA-based gene replacement therapy, in which cDNA is introduced into cells for reverse transcription and translation into protein by the cell's machinery. However, this is also highly problematic due to low efficiency of gene transfer, difficulty in delivering large genes (>5 kb), and the bypassing of certain biological processing systems[73]. This study concentrates on a third option: the increase of endogenous *SMAD*3 production from the WT allele using small molecules. This method holds the benefit of allowing for natural expression of all splice variants in appropriate tissue and normal posttranslational modifications.

An encouraging example of therapeutic pharmacologic modulation of a haploinsufficient disorder impacting the TGF-β pathway can be found in estrogen therapy for hereditary haemorrhagic telangiectasia (HHT), also known as Rendu-Osler-

Weber Syndrome. This autosomal dominant vascular disease is caused by haploinsufficiency of *Endoglin (ENG)* or *ALK1* genes, both of which code for proteins in the TGF-β pathway[74, 77]. HHT manifests as moderate to severe epistaxis (nosebleeds) caused by fragile telangiectases (spider veins) on the nasal mucosa[78]. In a study by Albiñana *et al*., raloxifene, a selective estradiol receptor modulator, significantly improved epistaxis in post-menopausal women with osteoporosis. *In vitro* raloxifene increased RNA and protein levels of *ENG and ALK1* at the endothelial cell surface, moderating haploinsufficiency. In functional assays this increase in expression translated to improved endothelial tubulogenesis and faster migration of cells after disruption of endothelial monolayers in wound-healing assays[74].

Another example of the use of small molecules to modulate haploinsufficiency is in a study by Zhang *et al*. on Williams-Beuren Syndrome and Supravalvular Aortic Stenosis, two disorders secondary to the heterozygous mutation of the elastin gene *ELN[73]*. The study used engineered zinc finger transcription factors to augment expression of intact WT *ELN* to compensate for haploinsufficiency of elastin protein. They found that the engineered zinc finger proteins were able to significantly increase both *ELN* RNA and protein in patient fibroblasts, as well as stimulate elastogenesis in bioengineered blood vessels. Moreover, as the induction of a gene cannot be targeted specifically to the WT allele, they address the concern of adverse effects from induction of the mutant allele. They found that concomitant activation of the mutant allele did not overwhelm the capacity of NMD to degrade mutant transcripts[73]. As it was previously shown that mutant transcripts in AOS patient fibroblasts are degraded by NMD[9], this

work provides support for chemical treatments that induce *SMAD3* gene expression in AOS.

Application to AOS

AOS patients begin developing aneurysms in childhood, although the exact age is difficult to estimate due to highly variable symptoms and the propensity for late diagnosis. Vascular remodeling is a result of a disturbance in the dynamic balance of VSMC ECM that favours degradation[13, 14]. Over time, loss of an organized elastin network causes remodeling of the ECM. This results in a stiffening of vessel walls, which tear and dissect under high-pressure blood flow. Despite *SMAD3* haploinsufficiency, tissues taken from AOS patients during surgery or autopsy show increased TGF-β signaling as well as increased levels of its downstream targets[9]. This may be due to a compensatory effort by TGF-β via both SMAD-mediated and alternative pathways in response to a deficiency in its downstream effector SMAD3. Elevated TGF-β signaling has also been found in other aneurysm disorders such as LDS (all types) and MFS; the former is caused by a gain of function mutation to TGF-β receptors, while the latter is caused by lack of sequestration of latent TGF-β by defective fibrillin proteins. Recently, excess TGF-β has been shown to be causative of pathogenic remodeling of VSMC ECM[18], suggesting it is the presence of excess TGF-β, and not a deficiency of SMAD3, that is driving vascular remodeling. Given this, we hypothesize that subsiding TGF-β compensation may have a therapeutic effect.

The basis of our therapy model is that restoring levels of functional SMAD3 using 13-CRA may be able to abrogate TGF-β compensation, in turn allowing ECM to return

to physiologic conditions. This theory relies on negative feedback from SMAD3 to TGF-β, which was shown to occur via phosphorylation of sites in the SMAD3 linker region by Millet *et al*. in 2009[79]. Theoretically, this should allow for the balance between deposition and degradation of ECM to be restored, which could prevent and even repair the progression of aneurysms. While in some cases it may be too late to completely reverse the dilatation that has already occurred, restoring elasticity to the vessel walls may be able to prevent further dissection and the likelihood of rupture. Because our study was done *in vitro*, whether 13-CRA will induce *SMAD3* in a general or tissue-specific manner is unknown. As dysregulation of the TGF-β/SMAD pathway has been associated with cancer[80, 81], additional studies using RNA sequencing to investigate the effects of increasing SMAD3 protein levels on other genes should be conducted *in vivo*.

C/EBPβ may play a role in mechanism of induction

Retinoids exert their effects through interaction with RARs and RXRs[66]. These ligand-inducible receptors heterodimerize and enter the nucleus where they interact with RAREs in gene promoter regions to exert transcriptional effects. As neither human nor mouse promoters contain any known RAREs, any inductive effect on *SMAD3* by retinoid molecules is likely indirect. This is supported by the finding that co-treatment with cyclohexamide, an inhibitor of protein translation, blocks *SMAD3* RNA induction[75]. An inability to induce transcription of *SMAD3* after exposure to a protein synthesis inhibitor indicates the necessity of one or more protein intermediates. Considering the relatively short time between dosing and transcript induction *in vitro*, we suspect a secondary or, at most, tertiary effect. We noted that the human *SMAD3* promoter contains

several transcription factor binding sites for CCAAT-enhancer-binding protein beta (C/EBPβ), and thus thought it a good candidate for a protein intermediate.

C/EBPβ is a bZIP domain transcription factor that has roles in differentiation and normal cell function in a number of tissues including osteocytes, adipocytes, hepatocytes, ovarian follicles, and mammary glands[70, 82-86]. In adipocytes, ceramide molecules (waxy lipids) have been shown to act on C/EBPβ in a biphasic manner[87]. After 4-16 hours of exposure, ceramides increase C/EBPβ phosphorylation and DNA binding ability and have no effect on C/EBPβ transcription (Appendix B). After longer exposures (24-48 hours), ceramides decrease C/EBPβ binding ability and nuclear localization[87]. We cultured NHF in a standard concentration of 200 nM 13-CRA in combination with 20, 40, and 60 μM of the ceramide N-acetyl-D-sphingosine for 8 hours to see if *SMAD3* induction could be blocked. We observed that addition of 60 μM of N-acetyl-D-sphingosine blocked induction of *SMAD3* RNA and protein, suggesting that C/EBPβ may play a part in the mechanism of *SMAD3* induction.

RA has been reported to potently inhibit C/EBPβ from activating its downstream targets by hampering DNA-binding ability in a mechanism that is not promoter-specific[75, 88]. It is therefore possible that C/EBPβ acts as a repressor of *SMAD3* transcription in a basal state and that the presence of 13-CRA alleviates this inhibition, resulting in *SMAD3* induction. Furthermore, given that short term exposure to ceramides has been shown to increase C/EBPβ DNA binding ability[87], one explanation for our observations is that 60 uM N-acetyl-D-sphingosine is sufficient to overcome the ability of RA to displace C/EBPβ from the *SMAD3* promoter. Further studies are needed to validate this theory and fully elucidate this mechanism.

Limitations

One limitation of our study was in exploring the effects of 13-CRA metabolites. 13-CRA has two biologically important metabolites: 9-cis-RA and all-trans-RA (tretinoin). While we would have liked to compare *in vitro* response to 13-CRA with 9-cis-RA, we were unable to obtain the latter compound. Second, due to widely variable pharmacokinetic information in the literature, we wished to measure post-dosing serum levels of 13-CRA and its metabolites *in vivo*. However, due to various limitations we were unable to perform these experiments. Given the differences in 13-CRA metabolism between mouse and human, future *in vivo* studies should measure serum levels of 13-CRA and corresponding protein induction for appropriate translation into clinical trials. Finally, our study contains the inherent limitations of Western blot quantification. While this semi-quantitative method is useful for visualizing changes in protein levels, the potential for film saturation provides a conceivable source of error. It is possible that for some experiments, changes in protein levels were outside the linear range of detection for our system. Future studies should establish a linear range of detection using known quantities of protein.

CONCLUSION AND FUTURE DIRECTIONS

In this study, we report the induction of *SMAD3* RNA and protein *in vitro* by 13-CRA. While this finding is not entirely novel, we are, to our knowledge, the first to show this relationship in VSMCs, and the first to suggest its application towards AOS. The lack of available treatment options for AOS patients underscores the importance of finding a

safe, low-cost therapy that may be both preventative and restorative. 13-CRA is a widely prescribed FDA-approved compound with minimal side effects. We have observed a variable, yet consistent trend in 13-CRA-induced *SMAD3* induction which may be of profound biological significance given the nature of haploinsufficient disorders.

Our lab has recently seen induction of *SMAD3* in cardiac tissue of WT mice using IP injection of 13-CRA[89]. We are currently experimenting with the use of bacon-flavoured 13-CRA 'cookies' that are made in-house with the desired 13-CRA concentration and can be dropped into a cage for oral consumption. This method is both less stressful for mice and provides a more accurate model for testing as 13-CRA is taken orally by patients. A *Smad3*+/- mouse model with AOS phenotype is currently available[90]. Once we have defined a dose-response curve, we hope to test 13-CRA efficacy in the disease model. Studies on these animals should attempt to begin treatment both very early in life and after aneurysm development to investigate the ability of 13-CRA to both prevent and reverse aortic remodeling. Following this, the next step will be to identify the 13-CRA concentration that optimally induces SMAD3 protein in healthy human subjects, possibly using leukocyte SMAD3 as a marker. Drawing blood from healthy subjects before and after administration of 13-CRA and isolating leukocyte protein would be a non-invasive way to do this. With the completion of this step, we would be very interested in partnering with clinicians in a trial of 13-CRA efficacy in AOS patients, bringing this finding to clinical application.

ACKNOWLEDGEMENTS

I would like to thank Dr. Hal Dietz and Dr. Elena Gallo MacFarlane at John Hopkins University for kindly providing VSMC lines.

Conflict of Interest statement: none declared.

FUNDING

Care for Rare funded by Genome Canada and CIHR.

REFERENCES

1. Orphanet. http://www.orpha.net/. 2015; Available from: http://www.orpha.net/.
2. Boycott, K.M., Alex, *Enhanced CARE for RARE Genetic Diseases in Canada*. 2012, Genome Canada: Ottawa, Ontario. p. 57.
3. WÄStfelt, M., B. Fadeel, and J.I. Henter, *A journey of hope: lessons learned from studies on rare diseases and orphan drugs*. Journal of Internal Medicine, 2006. **260**(1): p. 1-10.
4. Loeys, B.L., et al., *A syndrome of altered cardiovascular, craniofacial, neurocognitive and skeletal development caused by mutations in TGFBR1 or TGFBR2*. Nat Genet, 2005. **37**(3): p. 275-81.
5. Loeys, B.L.D., H.C., *Loeys-Dietz Syndrome*, in *GeneReviews*, A.M. Pagon RA, Ardinger HH, et al., Editor. 2008, University of Washington: Seattle (WA).
6. Viassolo, V., et al., *Fetal aortic root dilation: a prenatal feature of the Loeys-Dietz syndrome*. Prenat Diagn, 2006. **26**(11): p. 1081-3.
7. Malhotra, A. and P.L. Westesson, *Loeys-Dietz syndrome*. Pediatr Radiol, 2009. **39**(9): p. 1015.
8. Loeys, B.L., et al., *Aneurysm syndromes caused by mutations in the TGF-beta receptor*. N Engl J Med, 2006. **355**(8): p. 788-98.
9. van de Laar, I.M., et al., *Mutations in SMAD3 cause a syndromic form of aortic aneurysms and dissections with early-onset osteoarthritis*. Nat Genet, 2011. **43**(2): p. 121-6.
10. van de Laar, I.M., et al., *Phenotypic spectrum of the SMAD3-related aneurysms-osteoarthritis syndrome*. J Med Genet, 2012. **49**(1): p. 47-57.
11. Regalado, E.S., et al., *Exome sequencing identifies SMAD3 mutations as a cause of familial thoracic aortic aneurysm and dissection with intracranial and other arterial aneurysms*. Circ Res, 2011. **109**(6): p. 680-6.
12. Hilhorst-Hofstee, Y., et al., *An unanticipated copy number variant of chromosome 15 disrupting SMAD3 reveals a three-generation family at serious risk for aortic dissection*. Clin Genet, 2013. **83**(4): p. 337-44.
13. Thompson, R.W., *Reflections on the pathogenesis of abdominal aortic aneurysms*. Cardiovasc Surg, 2002. **10**(4): p. 389-94.
14. Isselbacher, E.M., *Thoracic and Abdominal Aortic Aneurysms*. Circulation, 2005. **111**(6): p. 816-828.
15. Lilly, L., *Pathophysiology of Heart Disease*. 2nd ed. 1997, Baltimore: Lippincott Williams & Wilkins.
16. Agmon, Y., et al., *Is aortic dilatation an atherosclerosis-related process? Clinical, laboratory, and transesophageal echocardiographic correlates of thoracic aortic dimensions in the population with implications for thoracic aortic aneurysm formation*. J Am Coll Cardiol, 2003. **42**(6): p. 1076-83.
17. Maleszewski, J.J., et al., *Histopathologic findings in ascending aortas from individuals with Loeys-Dietz syndrome (LDS)*. Am J Surg Pathol, 2009. **33**(2): p. 194-201.
18. Neptune, E.R., et al., *Dysregulation of TGF-beta activation contributes to pathogenesis in Marfan syndrome*. Nat Genet, 2003. **33**(3): p. 407-11.

19. Pyeritz, R.E. and V.A. McKusick, *The Marfan Syndrome: Diagnosis and Management*. New England Journal of Medicine, 1979. **300**(14): p. 772-777.
20. Lindsay, M.E. and H.C. Dietz, *Lessons on the pathogenesis of aneurysm from heritable conditions*. Nature, 2011. **473**(7347): p. 308-316.
21. Jones, K.B., et al., *Toward an understanding of dural ectasia: a light microscopy study in a murine model of Marfan syndrome*. Spine (Phila Pa 1976), 2005. **30**(3): p. 291-3.
22. Jones, J.A., F.G. Spinale, and J.S. Ikonomidis, *Transforming growth factor-beta signaling in thoracic aortic aneurysm development: a paradox in pathogenesis*. J Vasc Res, 2009. **46**(2): p. 119-37.
23. Ramirez, F., et al., *Fibrillin microfibrils: multipurpose extracellular networks in organismal physiology*. Physiol Genomics, 2004. **19**(2): p. 151-4.
24. Ramirez, F. and L. Pereira, *The fibrillins*. Int J Biochem Cell Biol, 1999. **31**(2): p. 255-9.
25. Dietz, H.C., et al., *Recent progress towards a molecular understanding of Marfan syndrome*. Am J Med Genet C Semin Med Genet, 2005. **139c**(1): p. 4-9.
26. Yu, L., M.C. Hebert, and Y.E. Zhang, *TGF-beta receptor-activated p38 MAP kinase mediates Smad-independent TGF-beta responses*. Embo j, 2002. **21**(14): p. 3749-59.
27. Dumont, N., A.V. Bakin, and C.L. Arteaga, *Autocrine transforming growth factor-beta signaling mediates Smad-independent motility in human cancer cells*. J Biol Chem, 2003. **278**(5): p. 3275-85.
28. Griswold-Prenner, I., et al., *Physical and functional interactions between type I transforming growth factor beta receptors and Balpha, a WD-40 repeat subunit of phosphatase 2A*. Mol Cell Biol, 1998. **18**(11): p. 6595-604.
29. Itoh, S., et al., *Elucidation of Smad requirement in transforming growth factor-beta type I receptor-induced responses*. J Biol Chem, 2003. **278**(6): p. 3751-61.
30. Wilkes, M.C., et al., *Cell-type-specific activation of PAK2 by transforming growth factor beta independent of Smad2 and Smad3*. Mol Cell Biol, 2003. **23**(23): p. 8878-89.
31. Arai, T., et al., *Genomic structure of the human Smad3 gene and its infrequent alterations in colorectal cancers*. Cancer Lett, 1998. **122**(1-2): p. 157-63.
32. Riggins, G.J., et al., *Mad-related genes in the human*. Nat Genet, 1996. **13**(3): p. 347-9.
33. Massague, J., *TGF-beta signal transduction*. Annu Rev Biochem, 1998. **67**: p. 753-91.
34. Derynck, R., R.J. Akhurst, and A. Balmain, *TGF-beta signaling in tumor suppression and cancer progression*. Nat Genet, 2001. **29**(2): p. 117-29.
35. Zhu, Y., et al., *Smad3 mutant mice develop metastatic colorectal cancer*. Cell, 1998. **94**(6): p. 703-14.
36. Sodir, N.M., et al., *Smad3 deficiency promotes tumorigenesis in the distal colon of ApcMin/+ mice*. Cancer Res, 2006. **66**(17): p. 8430-8.
37. Kjellman, C., et al., *Identification and characterization of a human smad3 splicing variant lacking part of the linker region*. Gene, 2004. **327**(2): p. 141-52.

38. Abdollah, S., et al., *TbetaRI phosphorylation of Smad2 on Ser465 and Ser467 is required for Smad2-Smad4 complex formation and signaling*. J Biol Chem, 1997. **272**(44): p. 27678-85.
39. Souchelnytskyi, S., et al., *Phosphorylation of Ser465 and Ser467 in the C terminus of Smad2 mediates interaction with Smad4 and is required for transforming growth factor-beta signaling*. J Biol Chem, 1997. **272**(44): p. 28107-15.
40. Schiffer, M., et al., *Smad proteins and transforming growth factor-beta signaling*. Kidney Int Suppl, 2000. **77**: p. S45-52.
41. Xu, L., Y.G. Chen, and J. Massague, *The nuclear import function of Smad2 is masked by SARA and unmasked by TGFbeta-dependent phosphorylation*. Nat Cell Biol, 2000. **2**(8): p. 559-62.
42. Tsukazaki, T., et al., *SARA, a FYVE domain protein that recruits Smad2 to the TGFbeta receptor*. Cell, 1998. **95**(6): p. 779-91.
43. Eppert, K., et al., *MADR2 maps to 18q21 and encodes a TGFbeta-regulated MAD-related protein that is functionally mutated in colorectal carcinoma*. Cell, 1996. **86**(4): p. 543-52.
44. Zhang, Y., et al., *Receptor-associated Mad homologues synergize as effectors of the TGF-beta response*. Nature, 1996. **383**(6596): p. 168-72.
45. Nakao, A., et al., *TGF-beta receptor-mediated signalling through Smad2, Smad3 and Smad4*. Embo j, 1997. **16**(17): p. 5353-62.
46. Liu, F., C. Pouponnot, and J. Massague, *Dual role of the Smad4/DPC4 tumor suppressor in TGFbeta-inducible transcriptional complexes*. Genes Dev, 1997. **11**(23): p. 3157-67.
47. Shi, Y., et al., *Crystal structure of a Smad MH1 domain bound to DNA: insights on DNA binding in TGF-beta signaling*. Cell, 1998. **94**(5): p. 585-94.
48. Liu, F., *Receptor-regulated Smads in TGF-beta signaling*. Front Biosci, 2003. **8**: p. s1280-303.
49. Lamb, J., et al., *The Connectivity Map: using gene-expression signatures to connect small molecules, genes, and disease*. Science, 2006. **313**(5795): p. 1929-35.
50. Layton, A., *The use of isotretinoin in acne*. Dermatoendocrinol, 2009. **1**(3): p. 162-9.
51. Chang, L.M. and M. Reyes, *A case of harlequin ichthyosis treated with isotretinoin*. Dermatol Online J, 2014. **20**(2).
52. Sporn, M.B. and D.L. Newton, *Chemoprevention of cancer with retinoids*. Fed Proc, 1979. **38**(11): p. 2528-34.
53. Kraemer, K.H., et al., *Prevention of skin cancer in xeroderma pigmentosum with the use of oral isotretinoin*. N Engl J Med, 1988. **318**(25): p. 1633-7.
54. Lee, J.S., et al., *Randomized placebo-controlled trial of isotretinoin in chemoprevention of bronchial squamous metaplasia*. J Clin Oncol, 1994. **12**(5): p. 937-45.
55. Bollag, W. and E.E. Holdener, *Retinoids in cancer prevention and therapy*. Ann Oncol, 1992. **3**(7): p. 513-26.
56. Lammer, E.J., et al., *Retinoic acid embryopathy*. N Engl J Med, 1985. **313**(14): p. 837-41.

57. Coberly, S., E. Lammer, and M. Alashari, *Retinoic acid embryopathy: case report and review of literature*. Pediatr Pathol Lab Med, 1996. **16**(5): p. 823-36.
58. Yang, Y., et al., *Determination of plasma and brain levels of isotretinoin in mice following single oral dose by high-performance liquid chromatography*. J Pharm Biomed Anal, 2005. **37**(1): p. 157-63.
59. Kalin, J.R., M.J. Wells, and D.L. Hill, *Disposition of 13-cis-retinoic acid and N-(2-hydroxyethyl)retinamide in mice after oral doses*. Drug Metab Dispos, 1982. **10**(4): p. 391-8.
60. Kerr, I.G., et al., *Pharmacology of 13-cis-retinoic acid in humans*. Cancer Res, 1982. **42**(5): p. 2069-73.
61. Nulman, I., et al., *Steady-state pharmacokinetics of isotretinoin and its 4-oxo metabolite: implications for fetal safety*. J Clin Pharmacol, 1998. **38**(10): p. 926-30.
62. BASF Canada, *Isotretinoin*, in *Pharma Ingredients and Services*. 2010: Mississauga, Ontario.
63. Roche Laboratories Inc., *Accutane*. 2010.
64. Brazzell, R.K. and W.A. Colburn, *Pharmacokinetics of the retinoids isotretinoin and etretinate. A comparative review*. J Am Acad Dermatol, 1982. **6**(4 Pt 2 Suppl): p. 643-51.
65. McLane, J., *Analysis of common side effects of isotretinoin*. J Am Acad Dermatol, 2001. **45**(5): p. S188-94.
66. Chambon, P., *A decade of molecular biology of retinoic acid receptors*. Faseb j, 1996. **10**(9): p. 940-54.
67. Rollman, O. and A. Vahlquist, *Oral isotretinoin (13-cis-retinoic acid) therapy in severe acne: drug and vitamin A concentrations in serum and skin*. J Invest Dermatol, 1986. **86**(4): p. 384-9.
68. Pendaries, V., et al., *Retinoic acid receptors interfere with the TGF-beta/Smad signaling pathway in a ligand-specific manner*. Oncogene, 2003. **22**(50): p. 8212-20.
69. Xiao, S., et al., *Retinoic acid increases Foxp3(+) regulatory T cells and inhibits development of Th17 cells by enhancing TGF- β -driven Smad3 signaling and inhibiting IL-6 and IL-23 receptor expression*. J Immunol, 2008. **181**(4): p. 2277-84.
70. Dingwall, M., et al., *Retinoic acid-induced Smad3 expression is required for the induction of osteoblastogenesis of mesenchymal stem cells*. Differentiation, 2011. **82**(2): p. 57-65.
71. Natsoulis G, P.C., Gollub J, P Eynon B, Ferng J, Nair R, Idury R, Lee MD, Fielden MR, Brennan RJ, Roter AH, Jarnagin K *Title Drug Matrix - In Vivo Rat Liver Affymetrix*
72. Nelson AM, Z.W., Gilliland KL, Zaenglein AL, Liu W, Thiboutot DM. , *Sebocytes and skin from severe acne patients treated with 13-cis retinoic acid*. 2008.
73. Zhang, P., et al., *Engineered zinc-finger proteins can compensate genetic haploinsufficiency by transcriptional activation of the wild-type allele: application to Willams-Beuren syndrome and supravalvular aortic stenosis*. Hum Gene Ther, 2012. **23**(11): p. 1186-99.

74. Albiñana, V., et al., *Estrogen therapy for hereditary haemorrhagic telangiectasia (HHT): Effects of raloxifene, on Endoglin and ALK1 expression in endothelial cells*. Thrombosis and Haemostasis, 2010. **103**(3): p. 525-534.
75. Marchildon, F., et al., *Transcription factor Smad3 is required for the inhibition of adipogenesis by retinoic acid*. J Biol Chem, 2010. **285**(17): p. 13274-84.
76. Kotterman, M.A. and D.V. Schaffer, *Engineering adeno-associated viruses for clinical gene therapy*. Nat Rev Genet, 2014. **15**(7): p. 445-51.
77. Abdalla, S.A. and M. Letarte, *Hereditary haemorrhagic telangiectasia: current views on genetics and mechanisms of disease*. J Med Genet, 2006. **43**(2): p. 97-110.
78. Shovlin, C.L. and M. Letarte, *Hereditary haemorrhagic telangiectasia and pulmonary arteriovenous malformations: issues in clinical management and review of pathogenic mechanisms*. Thorax, 1999. **54**(8): p. 714-29.
79. Millet, C., et al., *A negative feedback control of transforming growth factor-beta signaling by glycogen synthase kinase 3-mediated Smad3 linker phosphorylation at Ser-204*. J Biol Chem, 2009. **284**(30): p. 19808-16.
80. Reiss, M., *Transforming growth factor-beta and cancer: a love-hate relationship?* Oncol Res, 1997. **9**(9): p. 447-57.
81. Massague, J., *TGFbeta in Cancer*. Cell, 2008. **134**(2): p. 215-30.
82. Wiper-Bergeron, N., C. St-Louis, and J.M. Lee, *CCAAT/Enhancer binding protein beta abrogates retinoic acid-induced osteoblast differentiation via repression of Runx2 transcription*. Mol Endocrinol, 2007. **21**(9): p. 2124-35.
83. Darlington, G.J., S.E. Ross, and O.A. MacDougald, *The role of C/EBP genes in adipocyte differentiation*. J Biol Chem, 1998. **273**(46): p. 30057-60.
84. Schrem, H., J. Klempnauer, and J. Borlak, *Liver-enriched transcription factors in liver function and development. Part II: the C/EBPs and D site-binding protein in cell cycle control, carcinogenesis, circadian gene regulation, liver regeneration, apoptosis, and liver-specific gene regulation*. Pharmacol Rev, 2004. **56**(2): p. 291-330.
85. Sterneck, E., L. Tessarollo, and P.F. Johnson, *An essential role for C/EBPbeta in female reproduction*. Genes Dev, 1997. **11**(17): p. 2153-62.
86. Robinson, G.W., et al., *The C/EBPbeta transcription factor regulates epithelial cell proliferation and differentiation in the mammary gland*. Genes Dev, 1998. **12**(12): p. 1907-16.
87. Sprott, K.M., et al., *Decreased activity and enhanced nuclear export of CCAAT-enhancer-binding protein beta during inhibition of adipogenesis by ceramide*. Biochem J, 2002. **365**(Pt 1): p. 181-91.
88. Schwarz, E.J., et al., *Retinoic acid blocks adipogenesis by inhibiting C/EBPbeta-mediated transcription*. Mol Cell Biol, 1997. **17**(3): p. 1552-61.
89. Vanstone, D.J., *Personal communication*, S. Putos, Editor. 2015.
90. Dietz, D.H., *Personal communication*, A. MacKenzie, Editor. 2015.

APPENDICES

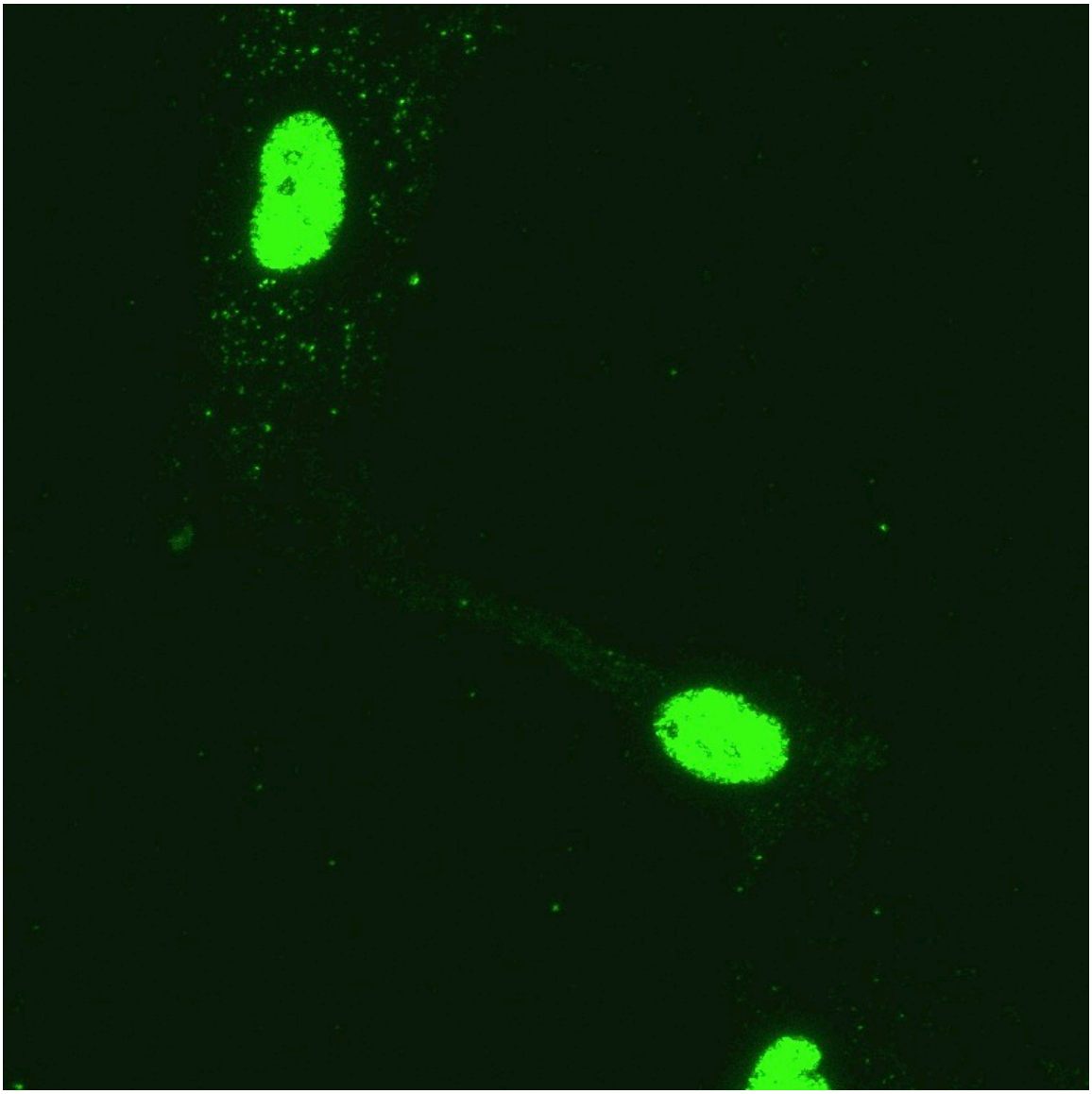

Appendix A. Immunofluorescent image of patient fibroblasts with SMAD3 visible in the cytoplasm.

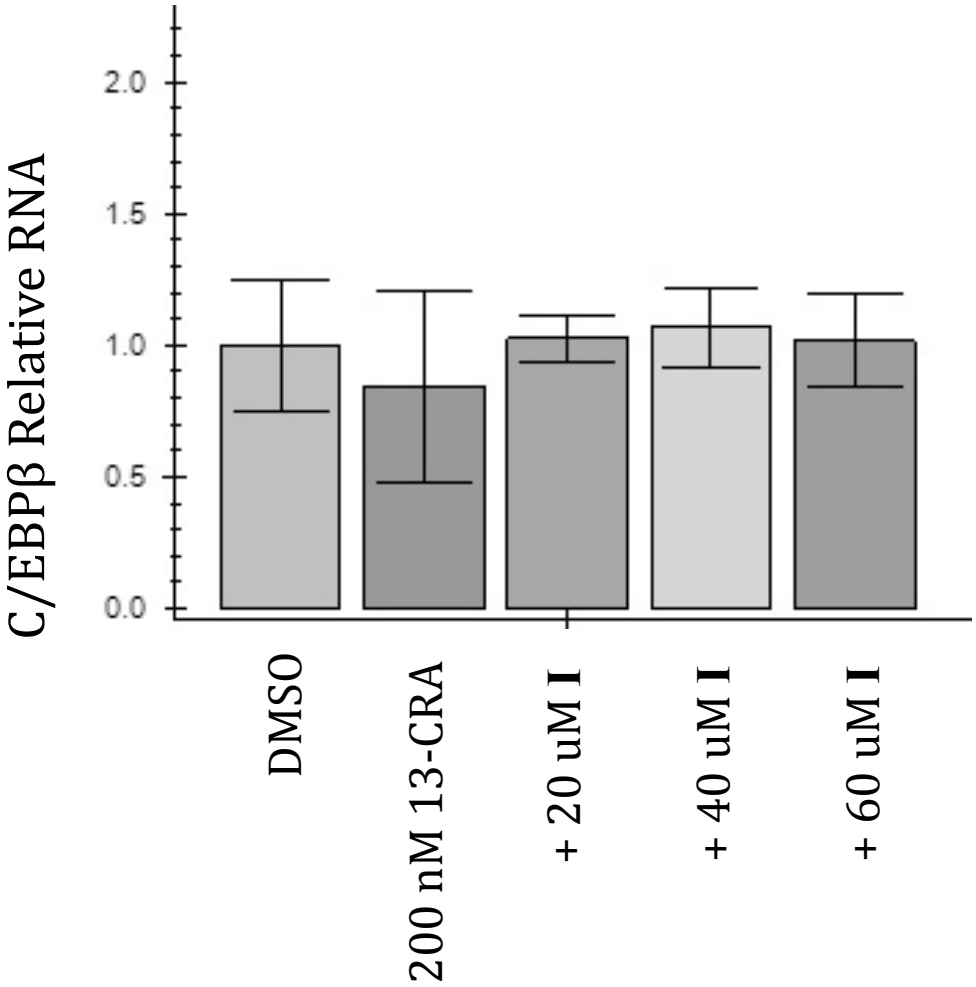

Appendix B. Unchanging C/EBPβ RNA in NHF in response to 200 nM 13-CRA and increasing levels of the C/EBPβ inhibitor N-acetyl-D-sphingosine after 8 hours. I=inhibitor. n=2. Error bars represent standard deviation. qPCR by Dr. Alan Mears.